Highly Sterically Encumbered Gold Acyclic Diaminocarbene Complexes: Overriding Electronic Control in Regiodivergent Gold Catalysis

Aaron A. Ruch,[†] Matthew C. Ellison,[†] John K. Nguyen,[†] Fanji Kong,[†] Sachin Handa,[‡,§] Vladimir N. Nesterov,[†] and LeGrande M. Slaughter*,[†]

[†]Department of Chemistry, University of North Texas, Denton, Texas 76203, United States

[‡]Department of Chemistry, Oklahoma State University, Stillwater, Oklahoma 74078, United States

Supporting Information Available

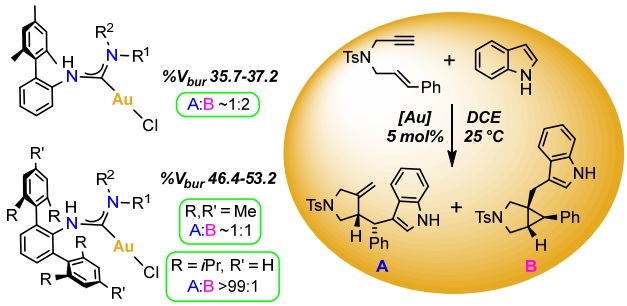

ABSTRACT: Two series of sterically encumbered gold(I)-acyclic diaminocarbene (ADC) complexes were prepared by reaction of mono- and dialkylamines with gold-bound 2-mesitylphenyl isocyanide (monomesityl series) and 2,6-dimesitylphenyl isocyanide (dimesityl series). X-ray crystal structures and solution ^{1}H NMR data showed that the ADC-gold complexes adopt major rotameric conformations with the bulky biaryl/terphenyl group and one alkyl group located syn to gold. This engenders substantial steric hindrance at the metal, as evidenced by percent buried volume (%V_{bur}) parameters of 35.7 – 37.2 for the monomesityl series and 46.4 – 52.4 for the dimesityl series. Modest out-of-plane distortions of the ADC *N*-substituents in the dimesityl series were attributed to attractive CH···π interactions between alkyl groups and mesityl rings on the basis of dispersion-corrected density functional theory calculations. Gold-catalyzed regiodivergent domino cyclization/hydroarylation reactions of a 1,6-enyne with indole revealed that the bulky biaryl/terphenyl substituents of the ligands exert a strong influence on product selectivity, with the bulkier dimesityl ADC-Au catalysts inducing a shift away from the cyclopropane-fused product toward the normally disfavored alkene product. Incorporation of a yet bulkier bis(2,6-diisopropylphenyl)-substituted terphenyl moiety into the ADC led to a gold catalyst that provided exclusive selectivity for the alkene product. Computational modeling suggested that bulky terphenyl groups hinder attack at the α carbon in the initially formed organogold intermediate, allowing steric effects to override the intrinsic electronic preference for the cyclopropane product.

INTRODUCTION

Gold(I) catalysts have garnered increasing attention from synthetic organic chemists in recent years due to their ability to generate complex molecular structures, including polycyclic carbo- and heterocycles, from readily accessible precursors.[1] Most gold-catalyzed reactions occur via initial π-activation of unsaturated bonds toward attack by internal or external nucleophiles, often followed by intricate further transformations.[2] These reactions are often susceptible to regiodivergent mechanistic pathways that lead to mixtures of isomeric products.[2a,3] In order to make these transformations synthetically useful, catalysts that selectively favor one isomeric product over another are highly desirable.[4] A number of studies have demonstrated that the regioselectivities of gold-catalyzed processes can be tuned by varying the ligand attached to gold.[5,6] Although ligand electronic effects are often invoked in these studies,[7] the interplay of ligand donicity with steric and other factors in gold catalysis has not been widely investigated,[8] limiting chemists' ability to rationally control selectivity in gold catalysis.[9,10]

Ligand scaffolds with readily modified structural features offer promise for harnessing ligand effects to achieve selective gold catalysis. Acyclic diaminocarbenes (ADCs), also known as nitrogen acyclic carbenes (NACs), represent a relatively underdeveloped ligand platform that could be useful in this regard.[11] Although ADCs can be synthesized and metalated by several routes,[11b] their formation via metal-templated addition of protic nitrogen nucleophiles to isocyanides has special advantages for catalyst tuning and optimization, as both the amine

and isocyanide components can be widely varied to generate structurally diverse arrays of ADC ligands (Figure 1).[12] We and others have utilized this approach to prepare libraries of ADC complexes for catalyst screening and optimization, with a focus on palladium(II)[13] and gold(I)[14] As well as being catalytically versatile, these metal ions are sufficiently electrophilic to activate isocyanides toward nucleophilic attack by amines under mild conditions, resulting in ADCs that are sufficiently robust to serve as ancillary ligands.[9a,12,15] This approach to catalyst discovery has yielded some notable successes, including several palladium cross-coupling catalysts that display high air/moisture stability[13a] and/or very high turnover numbers,[13b,e] and a number of highly enantioselective chiral gold(I)-ADC catalysts.[14e-h] In addition, a few promising hints of regioselectivity control have been reported for gold catalysts with ADC ligands.[14a,b,16-18]

Figure 1. Pertinent features of ADC ligands for catalysis

Discussions of the advantages of ADCs as ligands for catalysis have typically focused on their unique electronic properties. ADCs are believed to be stronger σ-donors than the related and widely studied cyclic diaminocarbenes (*N*-heterocyclic carbenes, NHCs)[19] as a result of their larger N-C-N angles and concomitantly reduced HOMO *s*-character,[20] but they also possess increased π-acceptor capability.[21,22] Another important consequence of the larger N-C-N angles of ADCs is that nitrogen substituents are placed closer to the metal (Figure 1), potentially engendering increased influence on the reactivity of a bound substrate through steric and/or noncovalent interactions. This structural feature has likely contributed to the success of chiral ADC ligands in achieving high enantioselectivities in certain gold-catalyzed transformations, despite the 180° bond angle separating the chiral ligand from the substrate binding site.[14e-h]

Given these considerations, we viewed ADC ligands as a promising platform for the construction of highly encumbered carbene ligands that could potentially exert steric influences on selectivity in gold catalysis. Ligand steric effects have received less attention than electronic effects in gold catalysis,[7-8] although a number of reports in the literature suggest that they can positively influence both selectivity and activity. Evidence for ligand-based steric control of diastereoselectivity[23] or regioselectivity[6e,k,n,24] in gold-catalyzed reactions has been reported in a few notable studies. Sterically encumbered biaryl- and bis(biaryl)phosphine ligands have been shown to provide higher turnover numbers (TON) and/or turnover frequencies (TOF) compared with less bulky ligands in gold-catalyzed nucleophilic additions to alkynes,[25] presumably by preventing formation of off-cycle geminally diaurated species.[26] The sterically encumbered NHC ligands IMes and IPr, characterized by large percent buried volume parameters (%V_{bur})[27,28] of 36.5 and 45.6 (Chart 1a), are widely used in gold catalysis and have enabled some of the best reported activities[5b,29] and selectivities.[6d,h,30] Gold complexes of NHC and related cyclic

Chart 1. Representative examples of sterically encumbered (di)aminocarbene ligands

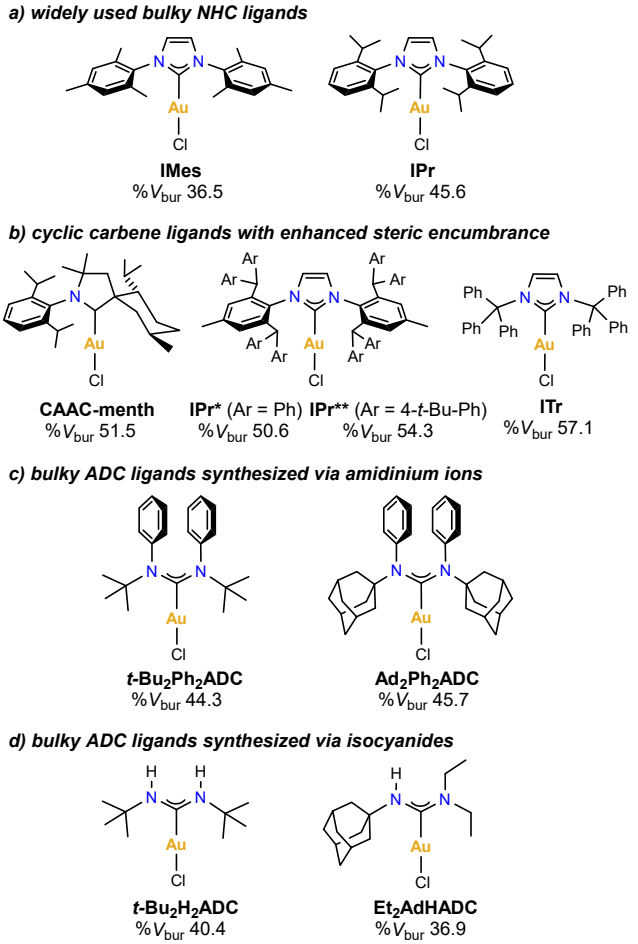

alkylaminocarbene (CAAC) ligands with greatly enhanced steric hindrance (%V_{bur} > 50), such as IPr*,[31] IPr**,[32] ITr,[33] and CAAC-menth[34] (Chart 1b), have been prepared, but investigations of their use in catalysis have so far been limited.[31b,32b,35] Hong and co-worker have provided precedent for highly bulky ADC ligands and their use in gold catalysis (Chart 1c),[16] although these were prepared from amidinium precursors rather than by the isocyanide route. Notably, the steric profile of Hong's Ad_2Ph_2ADC gold complex (%V_{bur} 45.7) is comparable to that of IPr.[36] Both Ad_2Ph_2ADC and *t*-Bu_2Ph_2ADC exhibit severe out-of-plane distortions of the ADC N-substituents in their L-AuCl complexes, and it was proposed that these distortions influence selectivity in regiodivergent catalysis.[16]

The isocyanide-based synthetic route offers potential advantages for the synthesis of very bulky ADC ligands. Synthetic routes based on deprotonation of formamidinium precursors can suffer from undesired side reactions of the relatively unstable free acyclic carbenes,[37] even when the carbene is protected by bulky groups.[38] In addition, synthetic routes to formamidinium ions from chloroiminium precursors are hampered by non-removable ammonium salt byproducts,[38a,39] and routes involving alkylation of *N*,*N*′-disubstituted formamidines are only feasible with methyl electrophiles,[18e,39-40] limiting the degree of steric bulk that can be attained. Hong's synthesis of amidinium precursors to Ad_2Ph_2ADC and *t*-Bu_2Ph_2ADC (Chart 1c) by reaction of chloroiminium salts with RN(SiMe$_3$)Ph obviates the problem of ammonium salt byproducts, but this procedure is

still predicated on the stability of the free carbene and has seen limited application.[16] Previous work suggests that the isocyanide route can tolerate significant steric encumbrance: several gold(I)-ADC complexes have been prepared from sterically hindered primary or secondary amines and correspondingly bulky isocyanides, as shown by the representative examples in Chart 1d.[14b,d] To the best of our knowledge, the *t*-Bu$_2$H$_2$ADC ligand[14d] exhibits the largest reported %V_{bur} (44.3)[28] of any structurally characterized ADC-Au^I complex yet prepared by this synthetic route.

A possible limitation of this approach is highlighted by previous studies showing that a high degree of steric strain in ADC ligands containing N-H groups can result in reversion of the carbene into amine and metal-isocyanide fragments.[41] Thus, achieving pronounced steric bulk comparable to that of IPr or Hong's Ad$_2$Ph$_2$ADC using the isocyanide route could be problematic. We hypothesized that the use of bulky biaryl[42] or *meta*-terphenyl[43] moieties as ligand building blocks could facilitate construction of new ADC ligands that have high levels of steric hindrance but avoid a detrimental degree of ligand distortion. These sterically encumbering aromatic ligand scaffolds can shield a significant portion of the coordination sphere, yet minimize severe intra-ligand or ligand-metal-ligand steric repulsions that could destabilize the ADC ligand by removing most of the steric bulk from the ligand plane.

Herein, we report a new family of sterically encumbered biaryl and terphenyl ADC-gold(I) complexes, some of which are characterized by extraordinarily large %V_{bur} parameters (%V_{bur}> 50). Steric tuning of the ADC ligands by variation of the biaryl/terphenyl and amine components has been shown to engender steric control of selectivity in a regiodivergent gold-catalyzed 1,6-enynye cyclization/indole addition reaction.[6c,d] In addition, rational modification of the steric bulk on the ADC ligand resulted in exclusive selectivity for the hydroarylation product resulting from remote attack of indole, overriding the intrinsic electronic preference for the isomeric product arising from indole attack alpha to gold.

RESULTS AND DISCUSSION

Syntheses. As synthons for highly bulky biaryl- and terphenyl-based ADC ligands, we initially chose 2-mesitylphenyl isocyanide **1** and 2,6-dimesitylphenyl isocyanide **2** (Scheme 1). These compounds were readily prepared from 2-bromoaniline and 2,6-dibromoaniline by a Suzuki coupling/formylation/dehydration sequence, following a procedure originally reported by Nagashima for related derivatives.[44] Figueroa's group has extensively developed the coordination chemistry of **2** and related bulky *meta*-terphenyl isocyanides as a means of stabilizing a variety of metals in low oxidation states and low coordination numbers.[45] Isocyanides **1** and **2** have not been previously utilized as precursors to carbene ligands.

The gold(I) chloride adducts of **1** and **2** were readily obtained via ligand substitution reactions with Au(THT)Cl[46] (Scheme 1). The different degree of steric shielding provided by the two isocyanides is evident in the solid-state structures of their complexes (Figure 2). *o*-Mesitylphenyl isocyanide complex **3** aggregates via aurophilic interactions[47] into cyclic tetramers, characterized by puckered-square Au$_4$ rings with Au···Au distances of 2.25 – 2.31 Å (Figure 2a).[48] By contrast, complex **4** forms two distinct crystalline polymorphs, both of which exhibit reduced aurophilic contacts. One polymorph (**4a**) is monomeric (shortest Au···Au distance 6.9 Å), and the other (**4b**) contains weak aurophilic dimers with Au···Au distances of 3.28 Å (Figure 2b). The increased bulk of the 2,6-dimesityl isocyanide ligand evidently blocks further aggregation of the dimers in **4b**.

Scheme 1. Synthesis of Sterically Encumbered Gold(I)-ADC Complexes

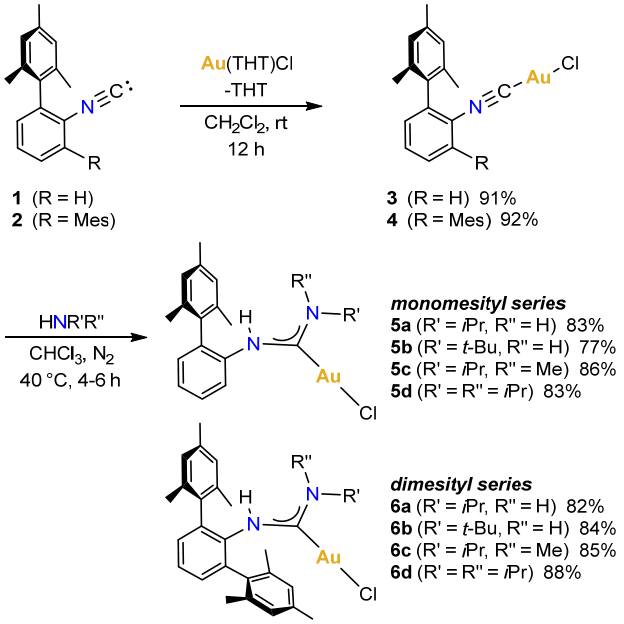

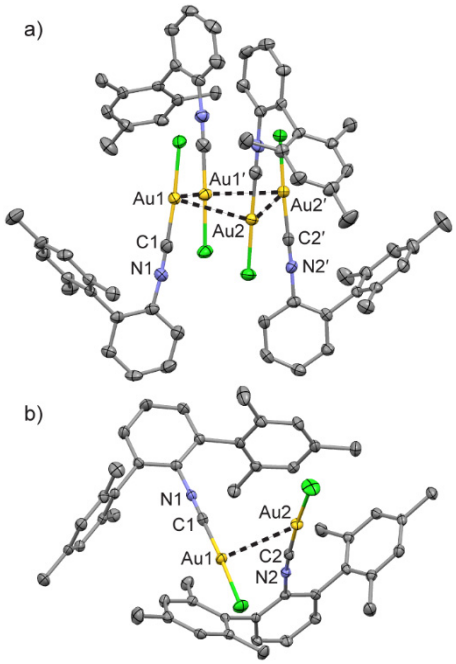

Figure 2. X-ray structures of Au(isocyanide)Cl complexes, showing assembly of **3** into tetramers (a) and **4** into dimers (b, polymorph **4a**) through aurophilic interactions. Selected bond distances: (a) **3**, Au1-Au1′ 3.254 Å, Au1-Au2 3.290 Å, Au2-Au2′ 3.290 Å; (b) **4a**, Au1-Au2 3.276 Å. For details of a second, crystallographically independent tetramer in the structure of **3** and a second polymorph of **4** (**4b**), see the Supporting Information.

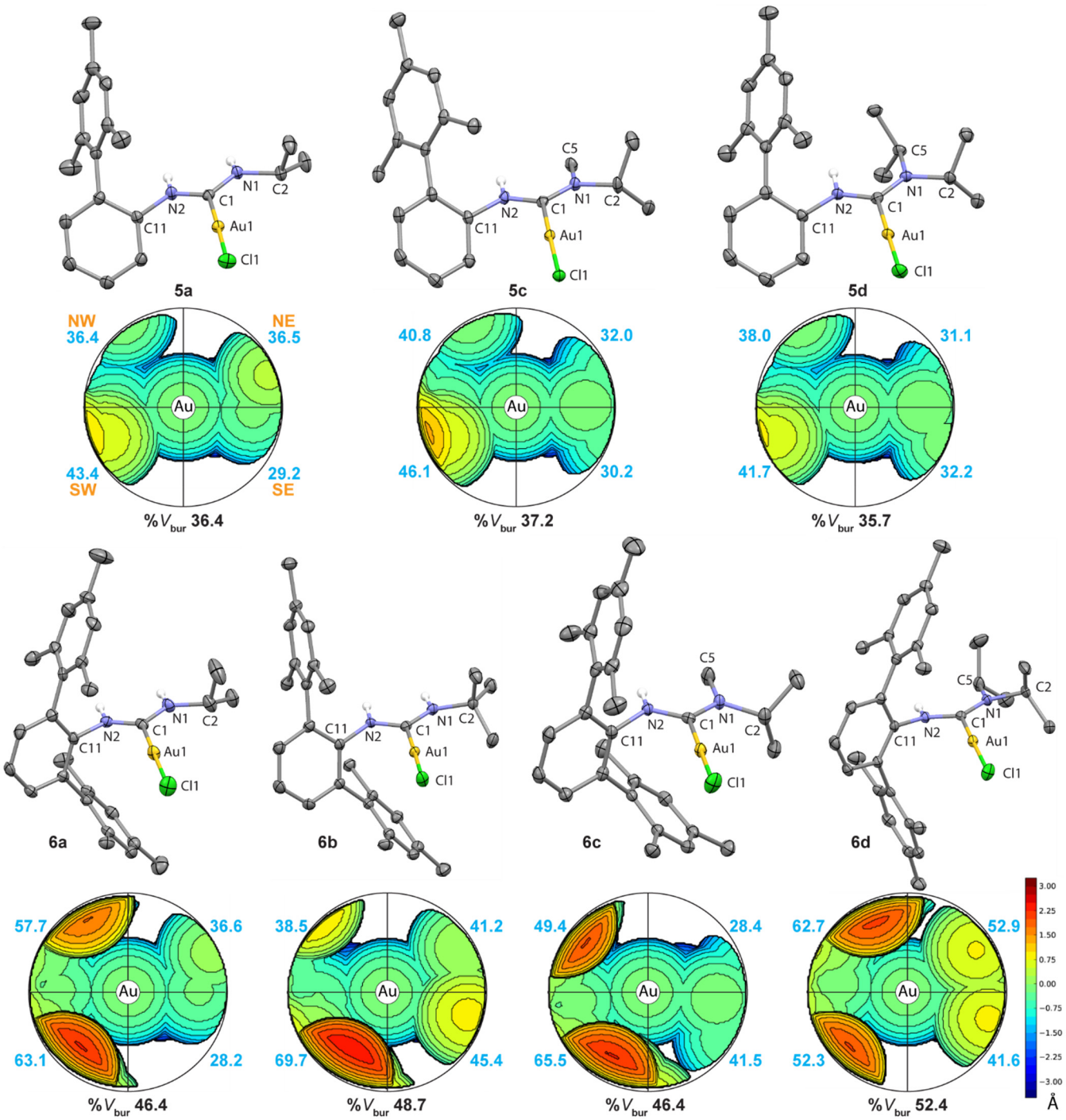

Figure 3. Ellipsoid plots (50% probability) and steric contour maps of the monomesityl and dimesityl series of Au(ADC)Cl complexes, derived from X-ray structures. Steric maps are drawn with Au,Cl and H atoms removed, and show only the portion of the ligand within the 3.5 Å radius sphere used to calculate %V_{bur} values. The overall %V_{bur} value for **6c** is an average for two crystallographically independent molecules in the crystal structure; the plot and quadrant %V_{bur} values depict only one of the two molecules (see the Supporting Information)

Table 1. Selected Bond Distances, Angles, and Torsion Angles for Au(ADC)Cl Complexes

	5a†	5c	5d	6a	6b	6c[a]	6d
Distances (Å)							
Au-$C_{carbene}$	1.991(2)	2.006(2)	2.005(2)	1.979(6)	1.984(2)	1.992(3)	2.001(2)
Au-Cl	2.2911(5)	2.2920(4)	2.2909(4)	2.298(2)	2.2876(5)	2.2846(8)	2.2928(5)
$C_{carbene}$-N1	1.326(3)	1.334(2)	1.328(2)	1.326(7)	1.330(3)	1.332(4)	1.334(2)
$C_{carbene}$-N2	1.340(3)	1.348(2)	1.349(2)	1.329(7)	1.345(3)	1.343(4)	1.345(2)
Angles (°)							
N1-C1-N2	115.7(2)	117.7(2)	116.8(2)	114.8(5)	115.1(2)	117.5(3)	119.2(2)
Au-C1-N1	122.9(2)	121.7(1)	123.5(1)	122.8(4)	125.4(2)	123.3(2)	123.2(1)
Au-C1-N2	121.3(2)	120.6(1)	119.6(1)	122.3(4)	119.3(1)	119.2(2)	117.4(1)
yaw angle[b]	0.8(1)	0.55(7)	1.95(7)	0.3(3)	3.1(1)	2.1(1)	2.90(7)
ADC substituent torsion angles (°)							
N1-C1-N2-C11	174.1(2)	176.4(2)	176.8(2)	177.2(5)[c]	166.8(2)	164.1(3)	166.5(2)[c]
N2-C1-N1-C2	-172.8(2)	176.6(2)	177.2(2)	-179.8(5)[c]	170.3(2)	-172.0(3)	-169.8(2)[c]
Aryl dihedral from NCN plane (°)[d]	130.9	124.5	129.9	93.9	109.3	96.3, 85.0[e]	83.7
C11 deviation from NCN plane (Å)	0.120(4)	0.078(3)	0.065(3)	0.059(10)	0.271(4)	0.330(4)	0.286(3)

[a]**6c** has two independent molecules per asymmetric unit; listed structural parameters are averages for the two distinct molecules, except as noted. [b]Yaw angle = [(Au-C1-N1)-(Au-C2-N2)]/2 (ref. 49). [c]Sign of torsion angle reversed for ease of comparison with other complexes. [d]Angles >90° signify that top of aryl ring (C12) is tilted away from Au. [e]Dihedral angles shown separately, as they differ for the two crystallographically independent molecules.

Both (isocyanide)gold(I) complexes reacted cleanly with a series of four primary and secondary alkyl amines of varying steric encumbrance [*i*PrNH$_2$, *t*-BuNH$_2$, *i*Pr(Me)NH, and *i*Pr$_2$NH] upon heating at 40 °C for 4-6 h in chloroform, affording two new series of Au^I(ADC)Cl complexes (Scheme 1). These are referred to herein as the monomesityl series (**5a-d**) and the dimesityl series (**6a-d**).

Structural and steric features of ADC ligands. X-ray crystal structures were obtained for all of the new Au^I(ADC)Cl complexes except **5b**, which did not form suitable crystals (Figure 3, Table 1). The ADC ligands in all seven structurally characterized complexes adopt similar stereoisomeric conformations, with the bulky aryl substituent on the isocyanide-derived nitrogen atom oriented *syn* to gold. For the ADCs synthesized from unsymmetrical amines (i.e. all except **5d** and **6d**), the larger of the two *N*-substituents on the amine-derived nitrogen atom is also located *syn* with respect to gold. Thus, the bulkiest parts of the ADC ligands are well positioned to impart steric shielding to the metal center as judged by the solid-state structures.

However, ^{1}H NMR spectroscopy revealed that two conformational isomers are present in CD_2Cl_2 solution for most of the Au-ADC complexes (Table 2). Only one conformer is observed for **5d**, **6c**, and **6d**; complexes **5a**, **5c**, **6a** and **6b** all exhibit two conformers, denoted **A** and **B**. A 1D-EXSY experiment with **5a** (see the Supporting Information) indicated that the two conformers are in a dynamic equilibrium at 25 °C, consistent with the well-known propensity of *N*-substituents in ADC ligands to undergo rapid exchange via hindered rotation about the C-N bonds.[14d,20a] The minor conformer (**B**), which is proposed to have the smaller amine substituent *syn* to gold, is only significant in the monomesityl ADC complexes derived from primary amines (**5a**,**b**), where its concentration in solution is ~50-80% that of **A** by ^{1}H NMR integration. For the other complexes, including the dimesityl ADCs derived from primary amines (**6a,b**), conformer **B** constitutes only up to 5-6% of the total concentration. Since the major conformer **A** corresponds to the geometry observed in the X-ray structures, the significant steric shielding evident in the solid state is likely to be a close reflection of the steric properties of the ADC ligands in solution for most of the complexes.

Complex **5b** is unique in this series in showing evidence of *four* different conformers in CD_2Cl_2 solution, including two in which the bulky biaryl group is in the "upper" position of the ADC ligand (see the Supporting Information). This is attributed to the bulky *tert*-butyl substituent, which is proposed to lower the barrier for hindered rotation about the $C_{carbene}$-N bonds through destabilizing steric interactions.

The (di)alkylamine units of the ADC ligands appear to exert subtly greater steric pressure within the Au-carbene plane than the bulky biaryl- or terphenyl groups, as judged by the

slightly larger Au-C-N angles on the alkyl side (Au-C-N_1, Table 1). This results in modest "yaw" angles[49] (Figure 4, Table 1) of 0.25 – 3.1° that push the bulky mesityl groups toward the gold centers. The slightly lesser steric pressure on the biaryl/terphenyl side of the ADCs can be attributed to the placement of the mesityl groups at the aryl *ortho* positions, which removes most of their substantial bulk from the Au-carbene plane.

Two of the monomesityl (ADC)AuCl complexes exist as aurophilic dimers in the solid state (**5a**,**d**; see Figure 5), whereas all of the dimesityl ADC complexes are monomeric. This provides further evidence of significantly larger steric hindrance in the dimesityl series of ADC ligands, as aurophilic interactions require a fairly close approach (typically ≤3.5 Å) of the two gold atoms.[47]

Table 2. Equilibrium Ratios of Au(ADC)Cl Conformers in CD_2Cl_2 Solution

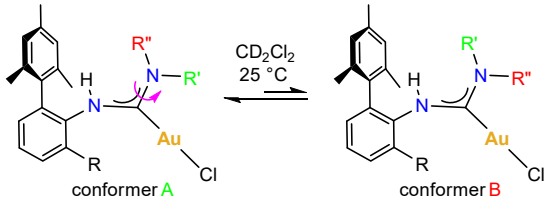

Complex	R′	R″	**A**:**B** ratio[a]
monomesityl series (R = H)			
5a	*i*Pr	H	66:34
5b	*t*-Bu	H	55:45[b]
5c	*i*Pr	Me	97:3
5d	*i*Pr	*i*Pr	N/A[c]
dimesityl series (R = Mes)			
6a	*i*Pr	H	95:5
6b	*t*-Bu	H	94:6
6c	*i*Pr	Me	100:0
6d	*i*Pr	*i*Pr	N/A[c]

[a]Determined by integration of ^{1}H NMR signals. [b]Two additional conformers observed (**A**:**B**:**C**:**D** ratios 43:35:12:10; see the Supporting Information. [c]Two conformers are degenerate (R′=R″=*i*Pr).

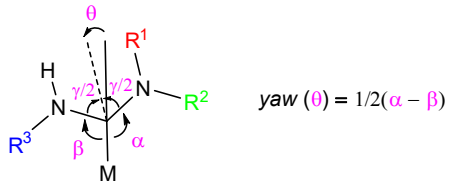

Figure 4. Definition of carbene yaw angle (ref. 49) as applied to ADC ligands.

The steric properties of the ADC ligands were assessed using the Percent Buried Volume (%V_{bur}) model, which represents steric bulk as the percentage of space occupied by the ligand within a sphere of r = 3.5 Å centered at the metal. This model has been developed extensively for the closely related NHC ligands due to its suitability for steric quantification of non-cone-shaped ligands.[27c,50] The %V_{bur} parameters derived from the X-ray structures[28] occupy the ranges of 35.7 to 37.2 for the monomesityl series and 46.4 to 52.4 for the dimesityl series (Figure 3). The combination of the bulky 2,6-dimesitylphenyl group with diisopropylamine endows **6d** with the bulkiest ADC ligand in the series (%V_{bur} 52.4). This ligand compares favorably with the extremely bulky NHC ligand IPr* (%V_{bur} 50.6, Chart 1b)[31] and Bertrand's highly encumbered CAAC-menth (%V_{bur} 51.5),[34] although it falls short of the yet more sterically encumbered NHCs IPr**[32] and ITr[33] (%V_{bur} 54.3 and 57.1, Chart 1b). All of the dimesityl ADC ligands in **6a-d** exhibit %V_{bur} parameters larger than those of Hong's tetrasubstituted *t*-Bu_2Ph_2ADC and Ad_2Ph_2ADC ligands (Chart 1c)[16] as well as those of other bulky ADCs prepared by the isocyanide route (e.g. *t*-Bu_2H_2ADC, %V_{bur} 40.4, Chart 1d).[14b,d]

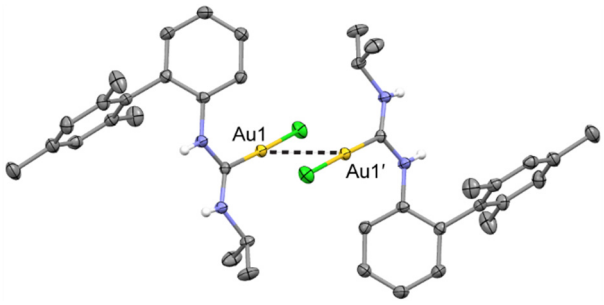

Figure 5. Centrosymmetric aurophilic dimer present in the X-ray structure of **5a** (Au1-Au1′ 3.26 Å). A similar dimer with a longer Au1-Au1′ distance (3.59 Å) is found in the structure of **5d** (Figure S9, Supporting Information)

A more detailed picture of the steric environment surrounding Au in each complex was gleaned by comparing the %V_{bur} contributions of individual quadrants in the steric maps of the ADC ligands (light blue numbers in Figure 3).[51] For both the monomesityl and dimesityl ADC complexes, the most hindered quadrants are located in the biaryl/terphenyl region. For the monomesityl complexes, the SW quadrant consistently contains the highest amount of bulk (%V_{bur} 41.1-46.1), corresponding primarily to the edge of the aryl ring opposite the mesityl group. The mesityl groups themselves contribute relatively little to the overall %V_{bur} of **5a**,**c**,**d**. The N-bound aryl ring in each of these complexes is rotated 125-131° with respect to the N-$C_{carbene}$-N plane of the ADC, evidently to minimize steric interactions between the mesityl *o*-CH_3 groups and the Au center (e.g. shortest Au···C_{Me} distance 4.12 Å for **5d**). This results in moderate steric bulk in the NW quadrants (%V_{bur} 36-41), which is not much greater than the bulk presented by the alkyl groups in the SE and SW quadrants (%V_{bur} 29.2-36.5).

For the dimesityl series, the presence of two *o*-mesityl substituents sterically prohibits the tilted aryl geometry seen in **5a**,**c**,**d**, instead favoring orientation of the central aryl rings at dihedral angles nearer to 90° with respect to the N-C-N plane (actual range 83.7° - 109.3°, Table 1) This causes a protrusion of steric bulk from the mesityl *o*-CH_3 groups into the coordination sphere of each dimesityl ADC complex, as shown by the large %V_{bur} contributions of the NW and/or SW quadrants (maximum %V_{bur} 62.7 – 69.7). Although the terphenyl groups of **6a-d** are still sufficiently tilted to remove some mesityl bulk

from one of the western quadrants, all of these complexes display short Au···C_{Me} distances involving the two nearest *o*-CH_3 groups (e.g. 3.64 Å and 3.65 Å for **6d**), illustrating the greater steric constraints present in this series compared with the monomesityl series.

The unusually large overall %V_{bur} parameter of 52.4 for the ADC ligand of **6d** can be attributed to a cooperative effect of the sterically demanding terphenyl group on the rotameric conformation of the alkyl substituents. Steric pressure forces the *i*Pr_2N unit of **6d** to adopt a geometry with the isopropyl -CH_3 groups facing toward gold, whereas the *i*Pr groups of **5a**, **5c**, **5d**, and **6a** are able to minimize steric repulsions by orienting away from gold. The resulting increase in steric shielding around Au is apparent in the alkyl region of the steric map of **6d** (Figure 3). Specifically, the %V_{bur} contributions of the NE and SE quadrants of **6d** (52.9 and 41.6) are significantly larger than the corresponding values for **5d** (31.1 and 32.2) and the other *i*Pr-substituted ADC complexes.

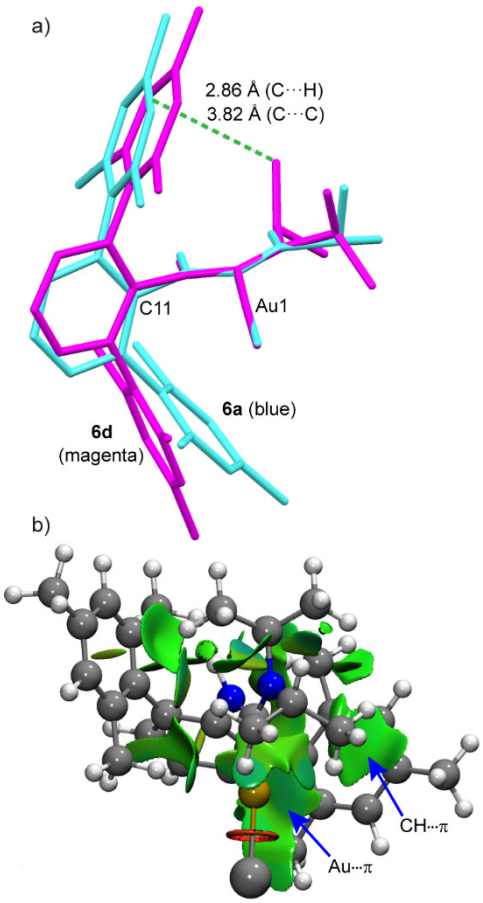

Figure 6. a) Overlay of the crystal structures of **6a** and **6d**, showing an apparent CH···π interaction and concomitant distortion of C11 out of the carbene plane; b) NCI plot of the DFT optimized structure of **6d** [BP86-D3/6-31+G* (main group),CEP-31G (Au)]. Green surfaces indicate weak noncovalent interactions. For a plot that differentiates weak attractive from weak repulsive interactions, see Figure S10 (Supporting Information).

The dimesityl ADC complexes **6b-d** display noticeable out-of-plane distortions of the ADC N-substituents in their X-ray structures. This is apparent in the torsion angles of 164.1 – 166.8° for the terphenyl *ipso* carbons (N1-C1-N2-C11), i.e., deviations of 13-16° from the ideal 180°, as well as in the lesser distortions involving the alkyl groups *syn* to gold (N1-C1-N2-C2 torsion angles 170-172°). The corresponding torsion angles are closer to 180° for the monomesityl series (Table 1). In addition, the absolute deviations of the N-bound carbon atoms from the N-C-N least-squares plane are larger for the dimesityl series (i.e. 0.27 – 0.33 Å for C11 in **6b-d**, versus 0.07 - 0.12 Å for the monomesityl series).

These distortions may serve to slightly relieve steric crowding of the mesityl *o*-CH_3 groups of **6b-d** with the ADC NH groups (avg shortest CH···HN distance 2.44 Å). This crowding is slightly greater in the less distorted ADC ligand of **6a** (avg shortest CH···HN distance 2.26 Å) and significantly less in the monomesityl analogues **5c** and **5d** (avg shortest CH···HN distance 3.29 Å). However, the ADC ligand distortions also appear to facilitate potentially attractive CH···π interactions[52] involving N-alkyl groups and one of the two mesityl rings, as illustrated by a C-H···C_{Ar} contact of 2.86 Å involving the "upper" isopropyl group in the crystal structure of **6d** (Figure 6a, magenta structure). The absence of an isopropyl group in this position in **6a** precludes this type of interaction, and no corresponding distortion of the ADC substituents is evident in **6a** (Figure 6a, blue structure).

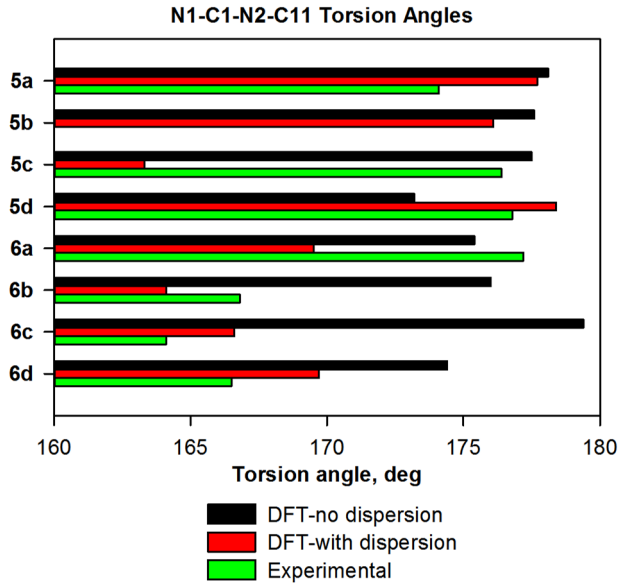

Figure 7. Comparison of experimental (X-ray) and DFT-calculated torsion angles indicating out-of-plane distortion of the biphenyl/terphenyl groups in Au(ADC)Cl complexes.

To gain insights into the possible role of attractive noncovalent interactions in the observed ligand distortions, we utilized density functional theory (DFT) to calculate optimized gas-phase geometries of all of the Au-ADC complexes, both with and without Grimme's empirical dispersion correction (D3).[53] This correction has been shown to improve modeling of noncovalent interactions derived from London dispersion forces.[54] A benchmarking study showed that the BP86 functional, in combination with the 6-31G* basis set for main group elements and the CEP-31G pseudopotential basis set for Au, reliably modeled important bond distances and angles within the ADC ligands (see the Supporting Information). Calculations

without the dispersion correction (BP86) produced ADC ligand geometries with very little out-of-plane distortion: the N1-C1-N2-C11 torsion angles are in the range of 173-179°, and no significant differences in these angles are apparent between the monomesityl and dimesityl series (Figure 7, black bars). Use of the dispersion-corrected functional (BP86-D3), however, reproduced the distortions observed in the X-ray structures of **6b-d** reasonably well, with calculated N1-C1-N2-C11 torsion angles in the range of 164-167° (Figure 7, green bars).

The BP86-D3-optimized structures of **6b-d** also exhibit CH···π contacts qualitatively similar to those seen in the X-ray structures (e.g. C-H···C_{Ar} contact of 3.03 Å in **6d**), although some of them involve different CH bonds or mesityl carbon atoms (Table 3). In addition, the central aryl rings of the terphenyl are rotated to a significantly larger degree in the BP86-D3-optimized structures (C1-N2-C11-C12 torsion angles 117-133°) than in the X-ray geometries (76 -118°). This appears to facilitate noncovalent Au···π interactions (e.g. Au···C_{ortho} 3.21 Å for one mesityl ring of **6d**, Table 3) that are not evident in the X-ray structures. Overall, the computational results support the idea that attractive noncovalent interactions contribute to the distortions observed in the dimesityl Au-ADC complexes, while also pointing out the difficulties of modeling such interactions in a large and complex ligand.

Table 3. Noncovalent interactions involving mesityl aromatic rings in Au(ADC)-Cl complexes

Complex	Interaction	Distance (Å)
X-ray structure		
6b	*t*-Bu -CH_2-H···centroid	4.30
6c[a]	*i*Pr -CH_2-H···C_{para}	2.96
	Me -CH_2-H···C_{ortho}	3.16
6d	*i*Pr -CH_2-H···C_{meta}	2.86
	*i*Pr2 -CH_2-H···C_{meta2}	3.37
DFT geometry[b]		
6b	*t*-Bu -CH_2-H···C_{meta}	2.89
	Au···C_{meta}[c]	3.25
6c	Me -CH_2-H··· C_{para}	2.95
	Me -CH_2-H··· C_{meta}	3.01
	Au···C_{ortho}[c]	3.26
6d	*i*Pr -CH_2-H··· C_{para}	3.03
	Au···C_{ortho}[c]	3.21

[a]Average values for two crystallographically independent but conformationally similar molecules of **6d**. [b]Gas phase geometries optimized using DFT [BP86-D3/6-31+G* (main group),CEP-31G (Au)]. [c]Comparable Au-π interactions do not occur in the X-ray structures, although some short alkyl CH···Au contacts (2.54 – 2.85 Å) are apparent in all of them.

Yang's method for visualization of noncovalent interactions,[55] as implemented in the NCIPLOT 3.0 program,[56] provided further evidence for attractive interactions in the DFT-optimized structure of **6d** (Figure 6b). Green surfaces represent regions in which the electron density indicates the presence of weak interactions.[55] The largest such regions in **6d** correspond to the C-H···π and Au···π interactions discussed above (Figure 6b). The attractive nature of these interactions was corroborated using a reported method (see Figure S10 Supporting Information).[57]

We postulate that some of the discrepancies between the observed and BP86-D3-modeled ligand distortions (e.g. in **6a**, Figure 7) may arise from crystal packing interactions, given that the rotation barriers of conjugated amino groups are typically small (~≤10 kcal mol^{-1}) and thus easily overcome even by weak forces.[20a,58] Nevertheless, both the solid-state X-ray and gas-phase BP86-D3 structures for **6b-d** suggest a greater propensity for the bulkier dimesityl ADC ligands to undergo torsional deformations, which is also likely to be the case in solution.

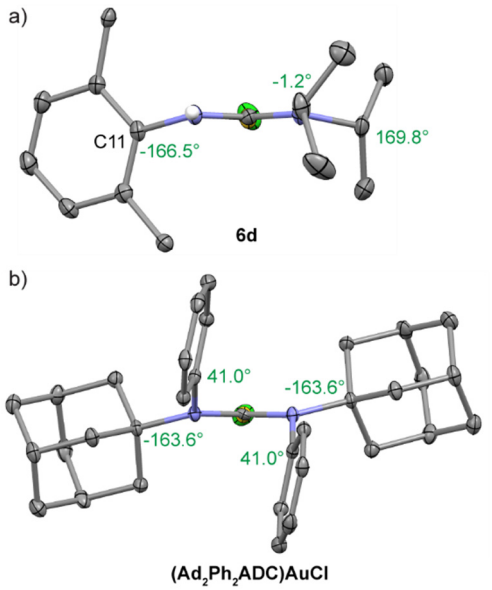

Figure 8. View along the carbene NCN planes for **6d** (only *ipso* carbons of mesityl rings shown for clarity) and Hong's Ad_2Ph_2ADC complex, showing out-of-plane distortions of substituents. Numbers in green are torsion angles relative to the N-$C_{carbene}$-N unit.

The out-of-plane distortions in the dimesityl ADC ligands of **6b-d** are markedly less than those seen in Hong's sterically demanding tetrasubstituted ADC ligands, *t*-Bu_2Ph_2ADC and Ad_2Ph_2ADC (Chart 1c),[16] despite **6b-d** having larger %V_{bur} parameters (Figure 3). The crystal structures of Hong's Au(ADC)Cl complexes show severe torsional displacements of the two phenyl groups on the "upper" positions the ADCs from the carbene N-C-N planes, with average N-$C_{carbene}$-N-C_{Ph} torsion angles of 36.0° for *t*-Bu_2Ph_2ADC and 41.0° for Ad2Ph2ADC (Figure 8). The bulky alkyl groups show more modest degrees of twist similar to those observed for the 2,6-dimesitylphenyl group in **6b-d**, with average N-$C_{carbene}$-N-C_{alkyl} torsion angles of 165.5° for ADC-*t*Bu_2Ph_2 and 163.6° for ADC-Ad_2Ph_2, corresponding to respective deviations of 14.5° and 16.4° from the ideal 180°. The pronounced distortions in Hong's ADCs appear to result primarily from a need to maximize favorable offset π-π interactions and minimize repulsive direct π-π interactions of the adjacent phenyl groups,[59] as proposed by the authors, although steric interactions of the large *t*-Bu and adamantyl groups with the Au atom may also play a

role.[16] By comparison with these and other sterically encumbered Au(ADC)Cl complexes,[14b,d] the dimesityl ADC complexes **6b-d** display a distinctive combination of large $\%V_{bur}$ and minimal to moderate out-of-plane distortions. We attribute this to a combination of factors: 1) steric bulk that is substantial but somewhat removed from the carbene ligand plane via the terphenyl framework; 2) the presence of no more than one hydrocarbyl substituent in the "upper" position of each ADC ligand, which limits both repulsive and attractive interactions involving these groups; 3) the lack of aryl groups on one side of the ADC, which precludes π-π interactions.

Catalytic Enyne Cyclization/Hydroarylation. The gold-catalyzed domino cycloisomerization/hydroarylation of 1,6-enyne **7** with indole (Table 4) is a well-studied regiodivergent reaction in which selectivity is known to be strongly dependent on the nature of the ancillary ligand.[6c,d] Previous studies have established that electronic control of regioselectivity is possible, with relatively weak-donor ligands such as triarylphosphites favoring the alkene product **8**[6c] and stronger donors such as NHCs favoring the cyclopropane product **9**.[6d,16,60] Given that the two products arise from indole attack at two different sites either adjacent to or remote from Au,[6c,d,16,60] we viewed this transformation as an ideal test reaction for evaluating steric control of regioselectivity with the new series of gold-ADC catalysts.

Table 4. Regiodivergent 1,6-Enyne Cyclization/Hydroarylation Catalyzed by Au-ADC complexes.[a,b]

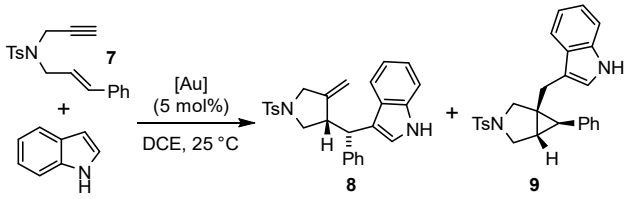

Precatalyst	Yield (%)[c]	**8**:**9** Ratio
monomesityl series		
5a	46	38:62
5b	64	34:66
5c	75	29:71
5d	75	34:66
dimesityl series		
6a	82	35:65
6b	84	44:56
6c	85	47:53
6d	88	44:56
refined catalyst		
13c	88	>99:1[d]

[a] Both products are racemic mixtures of enantiomers; only one enantiomer shown. [b] Reaction conditions: **7** (0.15 mmol), indole (0.17 mmol), catalyst (0.008 mmol), 25 °C, 3 h. [c]Isolated yield of inseparable mixture of **8** and **9** after silica gel chromatography. [d]**9** not detected in either crude or isolated product.

Active catalysts for the cyclization/hydroarylation of **7** with indole were generated by treating the Au(ADC)Cl complexes with $AgSbF_6$ in CH_2Cl_2 solution, followed by filtration through Celite. All of the catalysts yielded mixtures of the two isomeric products **8** and **9** in moderate to good yields, but significant changes in the **8**:**9** ratio were observed as a function of ADC ligand substituent (Table 4). The monomesityl series of Au-ADC catalysts favored the cyclopropane product, with **8**:**9** ratios varying from 38:62 for **5a** to 29:71 for **5c**. The least bulky dimesityl ADC complex (**6a**) gave a similar product ratio to the monomesityl catalysts (35:65), but the bulkier members of the series **6b-d** showed a shift toward lower selectivities, with **9** only slightly favored (product ratios 44:56 to 47:53). The product selectivities do not correlate smoothly with the overall steric bulk of the ADC ligands as represented by $\%V_{bur}$ (Figure 9). Rather, the monomesityl and dimesityl series of catalysts form two distinct clusters, with all of the monomesityl complexes giving **8**:**9** product ratios near 0.5 and all of the dimesityl complexes except **6a** giving closer to equal ratios of products.

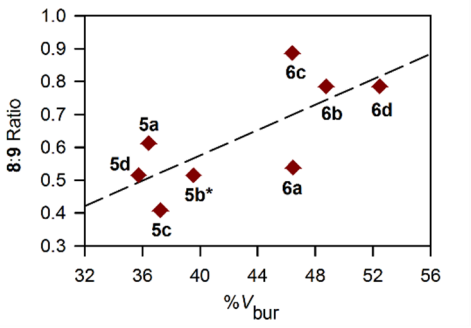

Figure 9. Enyne cyclization/hydroarylation product ratio versus $\%V_{bur}$ of the ADC ligand of the Au catalyst. *The $\%V_{bur}$ value of **5b** was calculated from the DFT optimized (BP86-D3) geometry; all others are derived from X-ray structures.

These results suggest that the alkyl substituents of the ADC ligands exert a lesser influence on product selectivity than the bulky aryl groups in the cyclization/hydroarylation of **7**. Specifically, the bulky terphenyl groups of the dimesityl ADCs appear to cause a shift in selectivity away from cyclopropane product **9** and toward alkene product **8**, with a net result of near-equal product ratios for this catalyst series.

Scheme 2. Proposed Intermediates in Gold-Catalyzed Enyne Cyclization/Hydroarylation

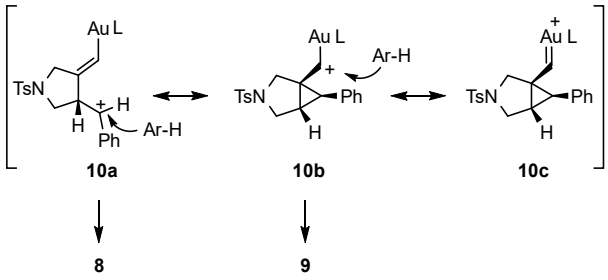

In the consensus mechanism for enyne cyclization/hydroarylation, product selectivity is determined by the site of indole attack on the proposed organogold intermediate **10** (Scheme 2).[6c,d,16,60] This intermediate can be viewed as lying on a continuum between a monocyclized gold vinyl species with a remote benzylic carbocation at the δ position (**10a**) and a bicyclic α-metallocarbenium species (**10b**); the latter is sometimes represented as a gold carbene (**10c**).[61] Attack at the gold-bound carbon (C_α) leads to the cyclopropane-containing product **9**, whereas alkene product **8** arises from remote indole attack at C_δ. Previous studies have attributed the observed selectivity for **9** with gold-NHC catalysts to the strong donicity of NHC ligands, which should relatively favor the α-carbocationic resonance form **10b**.[6d,16,60] ADC ligands might be expected to engender similar selectivities for **9**, given that they are proposed to be even stronger σ-donors than NHCs.[20] However, we hypothesize that the large terphenyl steric bulk of the dimesityl ADC-Au complexes is sufficient to hinder the attack of indole at C_α to some extent, counterbalancing the intrinsic electronic preference for **9**.

Catalyst Refinement for Optimization of Regioselectivity. We hypothesized that further steric blockage of C_α in intermediate **10** could lead to improved selectivity for alkene product **8**. To test this hypothesis, we sought to enhance the steric encumbrance of the ADC ligand platform by using $CNAr^{Dipp2}$ (**11**), a bulkier *m*-terphenyl isocyanide developed by Figueroa,[45c,d,45f-h,j] as a synthon. However, attempts to create a more hindered analogue of **6d** via reaction of $Au(CNAr^{Dipp2})Cl$ (**12**, Scheme 3) with HN*i*Pr$_2$ failed. NMR tube reactions in CD_2Cl_2, CD_3CN, $CDCl_3$, and DCE-d_4 showed no detectable Au-ADC product as monitored by ^{1}H NMR, even when **12** was heated with HN*i*Pr$_2$ for up to 3 d at 60°. We postulate that the high steric encumbrance of the $CNAr^{Dipp2}$ ligand either prevents its reaction with this relative hindered amine or results in an unstable ADC complex that immediately reverts to reactants.[41]

Scheme 3. Synthesis of Au(ADC)Cl Complex Containing the Sterically 2,6-Dipp$_2$Ph Group

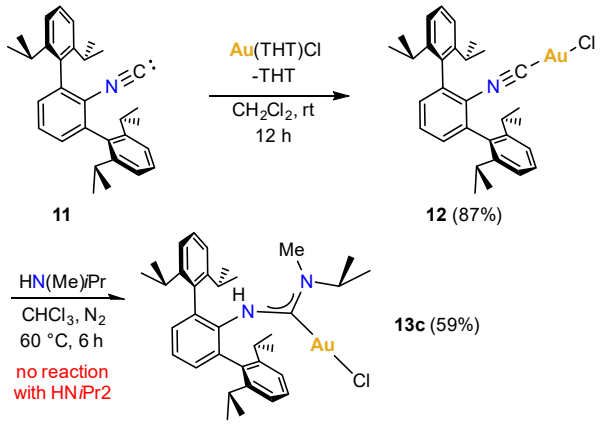

Remarkably, reaction of the only slightly less hindered amine *i*Pr(Me)NH with **12** led to formation of a stable, isolable ADC complex (**13c**). The X-ray structure of **13c** reveals significant effects of the bulkier terphenyl moiety on the structural features of the ADC ligand (Figure 10a). Steric pressure from the *o*-isopropyl groups, corroborated by short nearest Au···$C_{methine}$ distances of 3.50 Å and 3.53 Å (compared with Au···C_{Me} ≥ 3.64 Å for **6d**), enforces an almost perfectly perpendicular orientation of the central aryl ring of the terphenyl (C1-N2-C11-C12 torsion angle −89.5°). The carbene yaw angle is reduced nearly to zero for **13c** [0.4(2)°], further supporting increased steric pressure from the Dipp$_2$ -Ar group of **13c** compared to the Mes$_2$-Ar groups of **6b-d** (Table 1). Notably, the terphenyl and alkyl ADC substituents of **13c** show very little deviation from the N-$C_{carbene}$-N plane [relevant torsion angles: N1-C1-N2-C11 178.2(4)°, N2-C1-N1-C2 174.6(4)°], in contrast to the significant distortions seen in **6b-d** (Table 1, Figure 7). We attribute this to the sterically enforced symmetrical distribution of *i*Pr steric bulk on both sides of the N-C-N plane (i.e., left side of the steric map in Figure 10b), which prevents the terphenyl group from engaging in the types of noncovalent interactions that were identified as likely drivers of the distortions observed in **6b-d** (Figure 6, Table 3). Despite the noticeable influence of steric bulk on the ligand's structure, and the high steric hindrance (%V_{bur} >65%) present in the NW and SW quadrants of the steric map, the overall %V_{bur} parameter of 53.2% for the ADC ligand in **13c** is only modestly larger than that of the bulkiest dimesityl ADC complex, **6d** (%V_{bur} 52.4%).

With highly encumbered Au-ADC complex **13c** as the precatalyst, cyclization/hydroarylation reactions of **7** with indole displayed exclusive selectivity for the alkene product **8**, with no detectable formation of **9** (Table 4, last entry). To the best of our knowledge, no other reported catalyst has attained 100% selectivity for the alkene product in the hydroarylation of 1,6-enynes with indole.[6c,d,16,60] The highest reported **8**:**9** ratios in this reaction have been achieved with gold catalysts containing an electron-poor phosphite ligand (91:9)[6c,d] and a *p*-terphenyl phosphine ligand (95:5).[8]

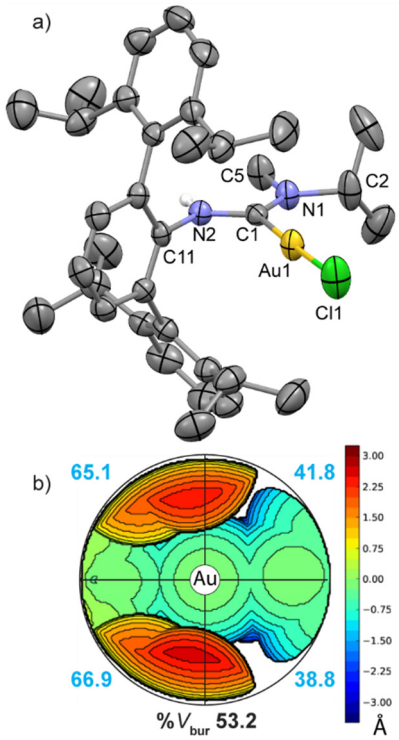

Figure 10. X-ray structure of complex **13c**: a) Ellipsoid plot (50% probability) and b) steric contour map. For detailed structural parameters, see the Supporting Information.

Discussion of Ligand Effects on Regioselectivity. Comparison of our results with those obtained by Hong and coworkers using the encumbered *t*-Bu$_2$Ph$_2$ADC and Ad$_2$Ph$_2$ADC ligands (Chart 1c)[16] are interesting. In the enyne cyclization/hydroarylation of **7** with indole, the *t*-Bu$_2$Ph$_2$ADC-Au catalyst was nonselective (51:49 ratio of **8**:**9**), whereas the bulkier Ad$_2$Ph$_2$ADC-Au catalyst favored the alkene product **8** by a 82:18 ratio. The authors suggested that the relative selectivities for **8**, in contrast to the predominant formation of **9** with Au-NHC catalysts,[6d,16,60] might be attributable to increased π-acceptor ability in the ADC ligands as a result of the large observed out-of-plane distortions (Fig. 8b) and consequent disruption of π-conjugation.[16] Increased π-backbonding was proposed to reduce the electron density at gold, thus disfavoring the α-carbocationic resonance form of the initial cyclization intermediate (**10b**, Scheme 2) and leading to preferential attack of the nucleophile at the δ carbon (i.e., via **10a**).

This electronic rationale for selectivity does not appear valid for our Au-ADC catalysts, however. Complexes **6b-d** provided similar **8**:**9** ratios to Hong's *t*-Bu$_2$Ph$_2$ADC-Au catalyst despite having much less distorted ADC ligands, and the highest selectivity for **8** was achieved with Dipp$_2$-substituted catalyst **13c**, which exhibits almost no out-of-plane distortion. In addition, there are only small differences in the observed metal-ligand bond lengths for the distorted dimesityl ADC complexes **6b-d** compared with their monomesityl counterparts (Table 1). The average Au-C$_{carbene}$ distance for **6c** and **6d** is only 0.010(2) Å longer than that for the monomesityl analogues **5c** and **5d**, while the corresponding difference in Au-Cl distances is even smaller at 0.003(1) Å. As Au-Cl distances are regarded as a useful measure of relative *trans* influence,[8,62] these data suggest very similar donor properties for all of the new ADC ligands.

Table 5. Selected Parameters Relevant to Gold-ADC Bonding

	δ ^{13}C:[a]	NBO charge:[b]		Calculated
Complex	C$_{carbene}$	Au	C$_{carbene}$	*d*(Au-Cl)[b]
5a	186.3	0.254	0.210	2.317
5b	187.6	0.252	0.212	2.320
5c	189.0	0.259	0.205	2.321
5d	189.3	0.263	0.208	2.323
6a	187.8	0.262	0.208	2.326
6b	188.4	0.253	0.214	2.327
6c	191.7	0.263	0.214	2.329
6d	192.0	0.248	0.218	2.334
13c	192.4	0.240	0.212	2.334

[a]Experimental values. [b]Calculated values [BP86/6-31+G* (main group),CEP-31G (Au)].

Experimental ^{13}C NMR data and DFT-calculated NBO charges show somewhat contradictory trends, with the dimesityl and DIPP$_2$ ADC complexes exhibiting modestly more downfield C$_{carbene}$ chemical shifts (by 1-3 ppm) but slightly lower calculated positive charges on Au, at least for **6d** and **13c**, versus the monomesityl series (Table 5). Calculated C$_{carbene}$ NBO charges do not support greater backbonding in the more encumbered Au-ADC complexes, instead predicting a slightly higher average positive charge (by 0.005) for dimesityl complexes **6a-d** versus monomesityl complexes **5a-d** (Table 5). There is a modest trend toward longer calculated Au-Cl bond lengths as steric encumbrance increases, which could be interpreted as reflecting changes in metal-carbene bonding.[8,62] However, the calculated Au-Cl values are almost identical for **6d** and **13c**, so this parameter does not correlate with the significant differences in selectivity seen between these two catalysts. Taken together, the data do not support the notion that sterically-induced electronic effects could be the origin of the observed selectivity differences in cyclization/hydroarylation of **7** observed with the bulky terphenyl ADC ligands.

DFT calculations on the proposed organogold intermediate **10** resulting from initial cyclization of **7** provided support for steric control of regioselectivity in the indole addition step. Geometry-optimized intermediates **10-5d**, **10-6d**, and **10-13c** all displayed structural features more closely resembling the C$_δ$-carbocation resonance form **10a** (Table 6), as judged by strong double-bond character in the C$_α$-C$_β$ bonds (*b*, 1.37 – 1.38 Å) and trigonal planar geometries about C$_δ$ (sum of bond angles 359.7-359.9°), although some incipient cyclopropane character was evident (C$_β$-C$_δ$, *d*, 1.96 – 2.01 Å). The similarity of bonding in all of these models provides further evidence that there are no significant electronic differences between the differently substituted ADC ligands.

Table 6. Selected Bond Lengths and Angles in DFT-Calculated Enyne Cyclization Intermediate (10) With Different ADC Ligands[a]

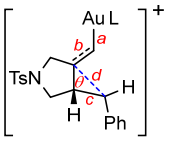

Complex[b]	*a*, Å	*b*, Å	*c*, Å	*d*, Å	*θ*, deg
10-5d	2.028	1.373	1.455	2.005	82.8
10-6d	2.030	1.376	1.453	1.957	80.3
10-13c	2.032	1.375	1.453	1.968	80.9

[a]DFT-optimized structures [BP86/6-31+G* (main group), CEP-31G (Au)]. [b]Intermediate **10** derived from complexes **5d**, **6d**, and **13c**.

A spacefilling plot of the optimized geometry of **10-6d** shows that, although the Au atom is well shielded by the 2,6-dimesitylphenyl and N*i*Pr$_2$ moieties, C$_α$ is not enclosed by these groups and remains largely exposed to attack (Figure 11a). In **10-13c**, by contrast, the *o*-*i*Pr substituents of the sterically encumbering DIPP$_2$-Ph moiety almost entirely block the approach to C$_α$, providing a simple explanation for the absence of product **9** in enyne cyclization/hydroarylation reactions catalyzed by **13c**. Notably, the site of attack leading to alkene product **8** (C$_δ$, green, Figure 13) is far removed from the ADC ligand and appears equally open to attack in all three calculated model intermediates (see the Supporting Information for additional views, including **10-5d**). Thus, the ability of catalyst **13c** to attain com-

plete selectivity for **8** can be attributed to extreme steric hindrance from the Dipp$_2$-phenyl group overriding an intrinsic electronic preference for attack at Cα. This steric control of selectivity is in contrast to the electronically-controlled preference for cyclopropane product **9** with the less hindered monomesityl series of Au-ADC catalysts **5a-d** and with previously reported catalysts containing NHC ligands that are similarly strong donors.[6d,16,60].

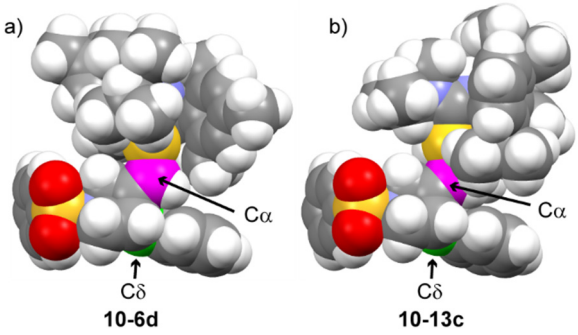

Figure 11. Spacefilling plots of DFT-optimized geometries [BP86/6-31+G* (main group), CEP-31G (Au)] of intermediates **10** derived from Au-ADC complexes (a) **6d** and (b) **13c**.

CONCLUSION

A family of nine gold(I) acyclic diaminocarbene complexes with large and tunable steric bulk was prepared via addition of protic amines to gold-bound biaryl and terphenyl isocyanides. The isocyanide-based synthetic approach was shown to be suitable for the construction of highly sterically encumbered carbene ligands, including some terphenyl ADC ligands with %V_{bur} parameters greater than 50%. These are comparable in overall steric hindrance to some of the bulkiest reported NHC ligands.[31-32,34] Structural studies revealed that conformations of the most hindered ADC ligands appear to result from an interplay of the steric properties of the different N-substituents. The bulky terphenyl moieties rotate to near-90° dihedral angles to minimize steric interactions of the outermost aryl groups with Au, while steric pressure within the Au-carbene plane forces both the terphenyl and the larger of the two amine substituents to adopt *syn* orientations relative to gold, resulting in substantial steric encumbrance adjacent to the metal coordination sphere. Slight out-of-plane distortions of the ADC N-substituents were attributed to noncovalent interactions of bulky aryl groups rather than to repulsive steric forces. These distortions are much smaller than those observed in previously reported bulky tetrasubstituted ADC-Au complexes,[16] despite the larger overall %V_{bur} parameters of the trisubstituted ADC ligands reported in this study. Computational, structural, and spectroscopic data do not support a significant change in the π-backbonding character of these ligands as a result of these minor distortions.

Studies of the effects of the ADC ligand structure on regioselectivity in the gold-catalyzed cyclization/hydroarylation of a 1,6-enyne with indole showed that product ratios were dependent primarily on the encumbrance of the bulky biaryl/terphenyl group, with the (di)alkyl amino groups exerting little influence. Replacing a 2-mesitylphenyl group with a bulkier 2,6-dimesitylphenyl group on the ADC ligand resulted in relatively modest changes in selectivity, from ~1:2 in favor of the cyclopropane product for the monomesityl series toward a ~1:1 ratio of alkene and cyclopropane products for the more hindered dimesityl series. By contrast, use of the yet more encumbered Dipp$_2$-phenyl-substituted catalyst **12c** caused a drastic shift in selectivity, affording exclusively the alkene product. This abrupt switch in selectivity could not have been predicted simply by comparing the %V_{bur} parameters of the series of ADC complexes, which showed only minor differences for catalysts with vastly different selectivities (i.e. %V_{bur} 52.4 for **6d** versus 53.2% for **13c**). These results imply that a global steric descriptor such as %V_{bur} may not be well-suited to capturing local changes in steric shielding at key reaction sites (in this case, Cα of intermediate **10**) that are crucial for tuning the selectivity of regiodivergent reactions.

In conclusion, this study demonstrates the value of a modular and readily tunable ligand framework that is compatible with highly encumbering groups in achieving highly regioselective gold catalysis. Given that carbene ligands typically favor the cyclopropane product in the chosen enyne cyclization/hydroarylation test reaction[6d,16,60] and that previous efforts to control regioselectivity in this reaction by tuning carbene ligand donor ability did not achieve selectivity for the alkene product,[60] the attainment of exclusive alkene selectivity with catalyst **13c** is a promising demonstration of the ability to override the intrinsic electron preference of a regiodivergent reaction though steric control.

EXPERIMENTAL SECTION

General Experimental Methods. All air-sensitive synthesis steps were performed under argon atmosphere using a vacuum line or under nitrogen atmosphere in a glovebox unless otherwise noted. All solvents for synthesis were dried and distilled immediately before use. Diethyl ether, benzene, pentane, and hexanes were dried over and distilled from sodium benzophenone ketyl. Chloroform, dichloromethane, and DCE were washed with a sequence of concentrated H_2SO_4, deionized water, 5% Na_2CO_3 and deionized water, followed by pre-drying over anhydrous $CaCl_2$, and were then refluxed over and distilled from P_2O_5 under nitrogen. NEt_3 was dried over activated 4 Å molecular sieves and then distilled, degassed, and stored over dried 4 Å sieves under nitrogen. CD_2Cl_2 was dried over and stored on activated 4 Å molecular sieves under vacuum and was vacuum-distilled before use. $Pd(PPh_3)_4$ (min. 99.5%, min. 9% wt/wt Pd) was purchased from Chem-Impex International, Inc. Au(THT)Cl[46] was synthesized from tetrachloroauric acid,[63] which was prepared from high-purity metallic gold (99.99%). 2′,4′,6′-trimethyl-[1,1′-biphenyl]-2-amine,[64] 2,6-Dimesitylphenyl isocyanide (**2**),[45a] and *N*-cinnamyl-4-methyl-*N*-(prop-2-yn-1-yl)benzenesulfonamide (**7**)[65] were synthesized according to literature procedures. All other reagents were obtained from Sigma-Aldrich or Acros in the highest available purity and used as received.

IR spectra were performed on Nujol mulls using a Nicolet 6700 FT-IR instrument. ^{1}H and ^{13}C NMR spectra were collected on Varian VNMRS (400 MHz and 500 MHz) and Varian Unity INOVA (600 MHz) FT-NMR spectrometers. Reported NMR chemical shifts were referenced to residual solvent peaks ($CDCl_3$: ^{1}H NMR, 7.26 ppm, ^{13}C NMR, 77.2 ppm; CD_2Cl_2: ^{1}H NMR, 5.32 ppm, ^{13}C NMR, 53.8 ppm).[66] Single crystal X-ray diffraction data were obtained on Bruker APEX II or Rigaku Oxford XtaLAB Synergy-S diffractometers. See the Supporting Information and deposited CIF files (CCDC 1945190-1945201) for details. Elemental analyses were performed by Midwest Microlab, Indianapolis, Indiana, or Complete Analysis Laboratories, Highland Park, NJ.

***N*-(2′,4′,6′-trimethyl-[1,1′-biphenyl]-2-yl)formamide.** To a stirred solution of 2′,4′,6′-trimethyl-[1,1′-biphenyl]-2-amine (1.56 g, 4.74 mmol) in 100 mL of benzene was added formic acid (95%, 2.68 ml, 71.0 mmol), and the reaction mixture was refluxed for 8 hours with periodic removal of water via a Dean-Stark apparatus. Upon completion of the reaction as monitored by TLC, the reaction mixture was added to deionized water and then extracted with EtOAc. The organic

layer was washed with saturated aqueous $NaHCO_3$ followed by drying over Na_2SO_4, and the EtOAc was then removed under reduced pressure. The resulting product was purified by flash column chromatography on silica (5:1 hexanes:EtOAc). R_f 0.44 (5:1 hexanes:EtOAc), white solid, mp = 173-175 °C, yield 1.02 g (90%). Mixture of two conformational isomers: major 58%, minor 42% by integration of ^{1}H NMR signals. ^{1}H NMR (600 MHz, $CDCl_3$): δ 8.74 (d, *J* = 11.5 Hz, 1H), 8.48 (d, *J* =7.8 Hz, 1H), 8.20 (s, 1H, CH minor), 8.19 (s, 1H, CH major), 7.39 (q, *J* = 7.8 Hz, 2H), 7.33 (d, *J* = 7.8 Hz, 1H), 7.24 (t, *J* = 7.8 Hz, 1H), 7.19 (t, *J* = 7.8 Hz, 1H), 7.13 (d, *J* = 7.8 Hz, 1H), 7.07 (d, *J* = 7.8 Hz, 1H), 7.00 (s, 2H) 6.97 (s, 2H), 6.94 (br s overlapped, 1H, NH minor), 6.81 (br s, 1H, NH major), 2.35 (s, 3H major), 2.33 (s, 3H minor), 1.96 (s, 6H major), 1.93 (s, 6H minor). ^{13}C NMR (151 MHz, $CDCl_3$): δ 161.4, 158.9, 138.3, 138.2, 137.1, 136.6, 134.7, 134.5, 133.0, 132.6, 131.0, 130.9, 129.8, 129.7, 129.0, 128.9, 128.6, 128.4, 125.2, 124.7, 120.7, 116.4, 21.19, 21.15, 20.3. IR (Nujol, cm^{-1}): ν 3268, 1693, 1661. Anal. calcd for $C_{16}H_{17}NO$: C, 80.30; H, 7.16; N, 5.85 %. Found: C, 80.38; H, 7.21; N, 5.90 %.

2-Mesitylphenylisocyanide (**1**). To a stirred solution of *N*-(2′,4′,6′-trimethyl-[1,1′-biphenyl]-2-yl)formamide (1 g, 4.19 mmol) and triethylamine (2.92 mL, 20.94 mmol) in CH_2Cl_2 (50 mL) at 0 °C under nitrogen was added freshly distilled $POCl_3$ (0.78 mL, 8.37 mmol). The reaction mixture was stirred and monitored by TLC until starting material had been consumed. The reaction mixture was then washed sequentially with water (2 x 100 mL), saturated aqueous $NaHCO_3$, and brine, and the organic layer was dried over Na_2SO_4. The CH_2Cl_2 solvent was removed under reduced pressure, and the product was purified by flash column chromatography on silica (4:1 hexanes:CH_2Cl_2). ^{1}H NMR (400 MHz, CD_2Cl_2): δ 7.51-7.46 (m, 2H), 7.41 (dt, *J* = 7.6 Hz, 1.6 Hz, 1H), 7.23 (dd, *J* = 7.6 Hz, 1.6 Hz, 1H), 6.99 (s, 2H), 2.34 (s, 3H) 1.97 (s, 6H). ^{13}C NMR (101 MHz, CD_2Cl_2): δ 166.0, 139.1, 138.2, 136.1, 134.3, 131.2, 129.9, 128.6, 128.4, 127.4, 126.4, 21.2, 20.2. IR (Nujol, cm^{-1}): 2118. Anal. calcd for $C_{16}H_{15}N$: C, 86.84; H, 6.83; N, 6.20 %. Found: C, 87.02; H, 6.83; N, 6.20 %.

Chloro(2-mesitylphenylisocyanide)gold(I) (3). 2-Mesitylphenylisocyanide **1** (131 mg, 0.90 mmol) and Au(THT)Cl (276 mg, 0.86 mmol) were dissolved in dry CH_2Cl_2 and allowed to stir for 12 h at 25 °C under nitrogen. The solvent was removed under reduced pressure, and the resulting product was washed with Et2O and purified by recrystallization from CH_2Cl_2/pentane. White crystalline solid, yield 354 mg (91%). ^{1}H NMR (400 MHz, CD_2Cl_2): δ 7.68-7.64 (m, 2H), 7.53-7.49 (m, 1H), 7.35-7.33 (m, 1H), 7.01 (s, 2H), 2.35 (s, 3H) 1.96 (s, 6H). ^{13}C NMR (151 MHZ, CD_2Cl_2): δ 142.8, 140.7, 139.1, 135.9, 132.6, 132.3, 131.9, 129.0, 128.96, 127.7, 124.3, 21.3, 20.2. IR (Nujol) 2234.8 cm^{-1}. Anal. calcd for $C_{16}H_{15}NAuCl$: C, 42.36; H, 3.33; N, 3.09%. Found: C, 42.65; H, 3.46; N, 3.09%.

Chloro(2,6-dimesitylphenylisocyanide)gold(I) (4). 2,6-Dimesitylphenylisocyanide **2** (201 mg, 0.589 mmol) and Au(THT)Cl (180 mg, 0.560 mmol) were dissolved in dry CH_2Cl_2 and allowed to stir for 12 h at room temperature under nitrogen. The solvent was removed under reduced pressure, and the resulting product was washed with Et_2O and purified by recrystallization from CH_2Cl_2/pentane. White crystalline solid, yield 294 mg (92%). ^{1}H NMR (400 MHz, CD_2Cl_2): δ 7.70 (t, *J* = 8 Hz, 1H), 7.33 (d, *J* = 8 Hz, 2H), 7.01 (s, 4H), 2.35 (s, 6H), 2.01 (s, 12H). ^{13}C NMR (101 MHz, CD_2Cl_2): δ 143.8, 140.9, 139.0, 135.8, 133.0, 132.2, 130.4, 129.0, 124.0, 21.3, 20.2. IR (Nujol, cm^{-1}): ν 2205 (m). Anal. calcd for $C_{25}H_{25}NAuCl$: C, 52.50; H, 4.41; N, 2.45 %. Found: C, 52.54; H, 4.39; N, 2.45%.

General procedure for synthesis of gold(acyclic diaminocarbene) chloride complexes. To a solution of chloro(2-mesitylphenylisocyanide)gold(I) **3** or chloro(2,6-dimesitylphenylisocyanide)gold(I) **4** (0.22 mmol) in $CHCl_3$ (2 mL) under a nitrogen atmosphere was added 2 equiv of neat amine. The reaction mixture was heated to 40 °C for 4-6 h. The progress of the reaction was monitored via TLC using basic alumina plates. Using 20-30% CH_2Cl_2 in hexanes as the eluent, the gold isocyanide complex could be observed as a mobile spot, while the Au(ADC)Cl product remained at the base of the TLC plate. After full conversion of the gold isocyanide complex, the reaction mixture was cooled to room temperature and filtered through Celite. Hexanes (3 mL) were added to precipitate the crude product as a white solid. The product was purified by recrystallization from CH_2Cl_2/pentane.

Chloro(*N*-2-mesitylphenyl-N′-isopropyldiaminocarbene)gold(I) (5a). White solid, yield 94 mg (83%). Mixture of two conformational isomers: major 70%, minor 30% by integration of ^{1}H NMR signals. R_f 0.22 (alumina, 4:1 hexanes/CH_2Cl_2). The product was purified by recrystallization from CH_2Cl_2/Et_2O. ^{1}H NMR (400 MHz, CD_2Cl_2): δ 8.40 (d, *J* = 8 Hz, 1H, minor), 8.24 (br s, 1H, minor), 7.48-7.44 (m, 2H major) 7.40-7.36 (m, 1H major, 1H minor), 7.28 (br s, 1H minor), 7.18-7.15 (m, 1H major), 7.05 (br s, 2H minor), 7.00 (s, 1H major), 6.97 (s, 2H major), 6.68 (d, J=5.6Hz, 1H minor), 6.60 (br s, 1H major), 6.38 (br s, 1H minor), 4.44 (br multiplet, 1H, major), 3.15 (septet, *J* = 7 Hz, 1H, minor), 2.33 (s, 3H, major), 2.30 (s, 3H, minor) 1.95 (s, 6H, minor), 1.92 (s, 6H, major), 1.22 (d, *J* = 4 Hz, 6H, major), 0.89 (d, *J* = 4 Hz, 6H, minor). ^{13}C NMR (101 MHz, CD_2Cl_2, four peaks in carbene/aromatic region not located due to apparent overlap of major/minor isomer peaks): δ 186.3, 138.7, 138.3, 137.5, 136.7, 135.9, 133.7, 133.3, 133.2, 133.0, 130.2, 129.1, 129.0, 128.5, 127.2, 125.6, 122.3, 105.13, 53.4, 45.2, 23.2, 21.5, 21.2, 21.1, 20.6, 20.5. Anal. calcd for $C_{19}H_{24}N_2AuCl$: C, 44.50; H, 4.72; N, 5.46 %. Found: C, 44.39; H, 4.67; N, 5.36%.

Chloro(*N*-2-mesitylphenyl-*N′*-*tert*-butyldiaminocarbene)gold(I) (5b). White solid, 89 mg (77%). Mixture of four conformational isomers: major A 43%, minor B 35%, minor C 12%, minor D 10% by integration of ^{1}H NMR signals. R_f 0.30 (4:1 hexanes: CH_2Cl_2). ^{1}H NMR (400 MHZ, CD_2Cl_2, -2 °C): δ 8.47 (d, *J* = 8 Hz, 1H major A, 1H minor B), 8.39 (d, *J* = 8 Hz, 1H minor C, 1H minor D), 8.25 (br s, NH, 1H, minor D), 8.23 (br s, NH, 1H, major A), 8.21 (br s, NH, 1H, minor B), 8.20 (br s, NH, 1H, minor C), 7.49-7.29 (m, 2H major A, 2H minor B, 2H minor C, 2H minor D), 7.31 (br s, NH, 1H minor C, 1H minor D), 7.18-7.10 (m, 1H major A, 1H minor B), 6.99 (s, 2H major A, 2H minor B, 2H minor C, 2H minor D), 6.96 (s, 1H, NH major A, minor B), 6.62 (br s,1H, NH, minor C, minor D), 6.47 (d, *J* = 8 Hz, 1H minor C, 1H minor D), 2.38 (s, 3H minor D), 2.34 (overlapped s, 3H minor B, 3H minor C), 2.31 (s, 3H major A), 1.96 (s, 6H major A), 1.92 (br s, 6H minor B), 1.88 (s, 6H minor C), 1.78 (s, 6H minor D), 1.57 (overlapped s, 9H minor C, 9H minor D), 1.53 (br s, 9H minor B) 1.00 (s, 9H major A). ^{13}C NMR (101 MHz, CD_2Cl_2, several peaks not located due to apparent overlap of major/minor isomer peaks): δ 187.6, 138.9, 138.3, 137.7, 136.9, 136.0, 133.5, 130.2, 129.2, 129.0, 128.5, 127.2, 122.1, 54.9, 31.2, 29.0, 21.2, 21.1, 20.6, 20.5. Anal. calcd for $C_{20}H_{26}N_2AuCl$: C, 45.59; H, 4.97; N, 5.32 %. Found: C, 45.92; H, 4.92; N, 4.93 %.

Chloro(*N*-2-mesitylphenyl-*N′*-isopropyl-*N′*-methyldiaminocarbene)gold(I) (5c). White solid, yield 100 mg (86%). Mixture of two conformational isomers: major 93%, minor 7% by integration of 1H NMR signals. Rf 0.20 (4:1 hexanes: CH_2Cl_2). 1H NMR (400 MHz, CD_2Cl_2): δ 8.35 (d, J = 8 Hz, 1H, major), 8.25 (d, J = 8 Hz, 1H, minor), 7.49-7.45 (m, 1H major, 1H minor), 7.40-7.36 (m, 1H major, 1H minor), 7.18 (dd, J = 4 Hz, 1H major, 1H minor), 7.00 (s, 2H major, 2H minor), 6.85 (br s, 1H major, 1H minor), 5.37-5.27 (m, 1H major), 3.51 (m, 1H minor), 3.46 (s, 3H, minor), 2.33 (s overlapped, 3H, major), 2.33 (s overlapped, 3H, major), 2.31 (s, 3H, minor), 1.97 (s overlapped/shoulder, 6H, minor), 1.96 (s, 6H, major), 1.22 (d, *J* = 8 Hz, 6H, major), 0.89 (d, *J* = 8 Hz, 6H, minor). ^{13}C NMR (101 MHz, CD_2Cl_2, six peaks in carbene/aromatic region not located due to apparent overlap of major/minor isomer peaks): δ 189.0, 138.6, 138.2, 136.7, 136.6, 134.1, 133.4, 130.3, 130.2, 129.1, 129.0, 128.7, 128.3, 127.1, 123.7, 123.6, 61.8, 48.8, 40.6, 27.7, 21.2, 21.1, 20.7, 20.44, 20.36, 19.1. Anal. calcd for $C_{20}H_{26}N_2AuCl$: C, 45.57; H, 4.98; N, 5.32 %. Found: C, 45.43; H, 4.88; N, 5.23 %.

Chloro(*N*-2-mesitylphenyl-*N′*,*N′*-diisopropyldiaminocarbene)gold(I) (5d). White solid, yield 102 mg (83%). R_f 0.27 (alumina, 4:1 hexanes/CH_2Cl_2). ^{1}H NMR (400 MHZ, CD_2Cl_2): δ 8.29 (d, *J* = 7.9 Hz, 1H), 7.44 (m, 1H), 7.36 (m, 1H), 7.11 (m, 2H), 6.98 (s, 2H), 5.38 (br s, 1H), 3.67 (sept, *J* = 7.3 Hz, 1H), 2.28 (s, 3H), 1.95 (s, 6H), 1.24 (d, *J* = 6.7 Hz, 6H), 0.84 (d, *J* = 7.3 Hz, 6H). ^{13}C NMR (101 MHz, CD_2Cl_2, only one set of *i*Pr peaks observed due to fluxionality): δ 189.3, 138.8, 138.7, 136.9, 134.0, 133.8, 130.1, 129.2, 128.2, 127.0, 123.8, 46.6, 21.1, 20.6, 20.0. Anal. calcd for $C_{22}H_{30}N_2AuCl$: C, 47.62; H, 5.45; N, 5.05 %. Found: C, 47.44; H, 5.52; N, 4.85 %.

Chloro(*N*-2,6-dimesitylphenyl-*N′*-isopropyldiaminocarbene gold(I) (6a). White solid, yield 90 mg (82%). Mixture of two conformational isomers: major 95%, minor 5% by integration of ^{1}H NMR signals. R_f 0.05 (3:2 hexanes:CH_2Cl_2). ^{1}H NMR (400 MHz, CD_2Cl_2): δ

7.56 (t, J = 7.6 Hz, 1H, major), 7.51 (br m, 1H, minor), 7.29 (d, J = 7.6 Hz, 2H, major), 7.26 (br s, 2H, minor), 6.99 (s, 4H, major), 6.94 (s, 4H, minor), 6.74 (br s, 1H, major), 6.66 (br s, 1H, minor), 5.93 (br m, 1H, minor), 5.71 (br s, 1H, major), 4.08 (septet, J = 6.5 Hz, 1H, major), 3.11 (multiplet, 1H, minor), 2.33 (s, 6H, major), 2.28 (s, 6H, minor), 2.17 (s, 12H, minor), 2.05 (s, 12H, major), 0.95 (d, J = 6.6 Hz, 6H, major), 0.81 (d, J = 6.4 Hz, 6H, minor). ^{13}C NMR (101 MHz, CD_2Cl_2, six peaks in carbene/aromatic region and two in aliphatic region not located due to apparent overlap of major/minor isomer peaks): δ 187.8, 139.1, 138.3, 137.7, 135.3, 134.4, 132.1, 131.6, 130.8, 129.6, 129.4, 128.9, 53.2, 22.7, 21.7, 21.2, 21.1, 21.0. Anal. calcd for $C_{28}H_{34}N_2AuCl$: C, 53.30; H, 5.43; N, 4.44 %. Found: C, 53.88; H, 5.49; N, 4.31 %.

Chloro(*N*-2,6-dimesitylphenyl-*N′*-*tert*-butyldiaminocarbene gold(I) (6b). White solid, yield 95 mg (84%). Mixture of two conformational isomers: major 94%, minor 6% by integration of ^{1}H NMR signals. R_f 0.06 (3:2 hexanes:CH_2Cl_2). ^{1}H NMR (400 MHz, CD_2Cl_2): δ 7.57 (t, J = 7.7 Hz, 1H major, 1H minor), 7.31 (d, J = 7.6 Hz, 2H, major), 7.27 (d, J = 7.6 Hz, 2H minor), 6.99 (s, 4H, major), 6.93 (s, 4H minor), 6.81 (s, 1H major, 1H minor), 5.99 (br s, 1H, major), 5.96 (overlapped/shoulder, 1H, minor), 2.32 (s, 6H, major), 2.28 (s, 6H minor), 2.06 (s, 12H major, ,12 H minor), 1.24 (s, 9H, major), 0.95 (s, 9H minor). ^{13}C NMR (101 MHz, CD_2Cl_2, four peaks in carbene/aromatic region not located due to apparent overlap of major/minor isomer peaks): δ 188.3, 140.3, 139.8, 138.2, 137.7, 135.3, 135.2, 134.3, 131.6, 130.7, 129.7, 129.69, 129.3, 129.1, 54.4, 32.0, 30.8, 29.3, 23.0, 21.2, 21.1, 14.2. Anal. calcd for $C_{29}H_{36}N_2AuCl$: C, 54.00; H, 5.63; N, 4.34 %. Found: C, 53.84; H, 5.67; N, 4.21 %.

Chloro(*N*-2,6-dimesitylphenyl-*N′*-isopropyl-*N′*-methyldiaminocarbene)gold(I) (6c). White solid, yield 96 mg (85%). R_f 0.16 (3:2 hexanes:CH_2Cl_2). ^{1}H NMR (400 MHz, CD_2Cl_2): δ 7.53 (t, J = 7.6 Hz, 1H major), 7.28 (d, J = 7.6 Hz, 2H major), 6.92 (s, 4H major), 6.34 (s, 1H, major), 4.83 (septet, J = 6.8 Hz, 1H, major), 2.30 (s, 6H, major), 2.28 (s, 3H, major), 2.20 (br s, 12H, major), 0.87 (d, J = 6.8 Hz, 6H, major). ^{13}C NMR (101 MHz, CD_2Cl_2,): δ 191.7, 140.6, 137.5, 136.4, 135.9, 135.2, 130.7, 128.72, 128.67 (br), 60.5, 26.9, 21.8 (br), 21.0, 19.8. Anal. calcd for $C_{29}H_{36}N_2AuCl$: C, 54.00; H, 5.63; N, 4.34 %. Found: C, 53.89; H, 5.68; N, 4.43 %.

Chloro(*N*-2,6-dimesitylphenyl-*N′*,*N′*-diisopropyldiaminocarbene gold(I) (6d). White solid, yield 103 mg (88%). R_f 0.13 (3:2 hexanes:CH_2Cl_2). ^{1}H NMR (400 MHz, CD_2Cl_2): δ 7.55 (t, J = 7.6 Hz, 1H), 7.28 (d, J = 7.6 Hz, 2H), 6.96 (br s, 2H), 6.86 (br s, 2H), 6.54 (br s, 1H, NH), 4.88 (br s, 1H), 3.47 (m, 1H), 2.48(s, 6H), 2.26 (s, 6H), 1.93 (s, 6H), 0.96 (d, J = 6.8 Hz, 6H), 0.85 (d, J = 7.2 Hz, 6H). ^{13}C NMR (101 MHz, CD_2Cl_2, 3 °C): δ 192.0, 140.9, 137.5, 135.5, 134.8, 130.6, 129.3, 128.9, 128.1, 46.0, 23.1 (br), 21.1 (br), 21.0, 20.6 (br), 20.5. Anal. calcd for $C_{31}H_{40}N_2AuCl$: C, 55.32; H, 5.99; N, 4.16 %. Found: C, 55.25; H, 5.82; N, 4.31 %.

Chloro[2,6-bis(2,6-diisopropylphenyl)phenylisocyanide]gold(I) (12). A solution of $CNAr^{Dipp2}$ **11** (200 mg, 0.47 mmol) and Au(THT)Cl (145 mg, 0.45 mmol, 0.95 equiv.) in dry CH_2Cl_2 (2 mL) was placed in a reaction vial under nitrogen atmosphere inside a glovebox. The vial was sealed and removed from the glovebox, and the reaction mixture was stirred at 25 °C overnight. The reaction mixture was then filtered through Celite, and hexanes were added to precipitate the crude product as a white solid. The product was purified by recrystallization from CH_2Cl_2/hexanes. White solid, yield 270 mg (87%). R_f 0.30 (2:1 hexanes:CH_2Cl_2). ^{1}H NMR (500 MHz, CD_2Cl_2) δ 7.71 (t, J = 7.7 Hz, 1H), 7.47 (t, J = 7.8 Hz, 2H), 7.40 (d, J = 7.7, 1.0 Hz, 2H), 7.31 (d, J = 7.8Hz, 4H), 2.47 (septet, J = 6.8 Hz, 4H), 1.14 (dd, J = 6.8 Hz, 6.9 Hz, 24H). ^{13}C NMR (126 MHz, CD_2Cl_2) δ 146.8, 144.6, 140.7, 133.2, 131.5, 130.6, 130.2, 124.9, 123.8, 31.5, 24.6, 24.2. Anal. calcd for $C_{31}H_{37}NAuCl$: C, 56.75; H, 5.68; N, 2.13 %. Found: C, 56.64; H, 5.69; N, 2.16 %.

Chloro[N-2,6-bis(2,6-diisopropylphenyl)phenyl-N'-isopropyl-N'-methyldiaminocarbene]gold(I) (13c). A solution of $Au(CNAr^{Dipp2})Cl$ (50 mg, 0.075 mmol) in $CHCl_3$ (1.0 mL) was placed in a reaction vial under nitrogen atmosphere inside a glovebox. The vial was sealed with a septum cap and removed from the glovebox, and *i*PrMeNH (16 μL, 0.150 mmol, 2 equiv) was added via microsyringe. The reaction mixture was then heated to 60 °C for 6 h. After consumption of the gold isocyanide complex as monitored by TLC, the reaction mixture was cooled to room temperature and filtered through Celite. Hexanes were added to precipitate the crude product as a white solid. The product was purified by recrystallization from CH_2Cl_2/hexanes. Mixture of two conformational isomers: major 95%, minor 5% by integration of ^{1}H NMR signals. R_f 0.30 (4:1 hexanes: CH_2Cl_2). Yield 32 mg (59%). ^{1}H NMR (500 MHz, CD_2Cl_2; visible minor isomer peaks noted; others overlapped or not visible) δ 7.56 (t, J = 7.6 Hz, 1H, major), 7.38 – 7.32 (m, 4H, major), 7.22 (d, J = 7.8 Hz, 4H, major), 6.23 (s, 1H, major), 4.92 (septet, J = 6.6 Hz, 1H, major), 3.11 (s, 3H, minor) 2.90 (br s, 4H, major), 2.24 (s, 3H, major), 1.32 (d, J = 6.8 Hz, 12H, major), 1.30 (d J = 5.4 Hz, 12H, minor), 1.28 (d J = 3.3Hz, 12H, minor) 1.06 (d, J = 6.6 Hz, 12H, major), 0.87 (d, J = 5.9 Hz, 6H, major), 0.73 (d, J = 6.6 Hz, 6H, minor). ^{13}C NMR (101 MHz, CD_2Cl_2; minor isomer peaks not visible) δ 192.5, 147.3, 141.0, 136.9, 135.7, 131.7, 128.9, 128.5, 123.4, 60.8, 31.6, 27.3, 26.2, 24.5, 19.9. Anal. calcd for $C_{35}H_{48}N_2AuCl$: C, 57.65; H, 6.63; N, 3.84 %. Found: C, 57.50; H, 6.56; N, 3.75 %.

Gold-catalyzed 1,6-enyne cyclization/hydroarylation. The gold catalyst $[(L)Au]^+[SbF_6]^-$ was freshly prepared by stirring (L)AuCl (3.8-5.1 mg, 5 mol%) and $AgSbF_6$ (2.6 mg, 5 mol%) in DCE (1.0 mL) for 15 min in a reaction vial inside a nitrogen-filled glovebox. The mixture was then passed through a 1.0 cm pad of Celite in a glass Pasteur pipet, and the filtrate was added to a solution of *N*-cinnamyl-4-methyl-*N*-(prop-2-yn-1-yl)benzenesulfonamide (**7**) (50 mg, 0.15 mmol) and indole (20 mg, 0.17 mmol) in 1.0 mL of dry DCE under nitrogen atmosphere. The vial was sealed with a septum cap, and the reaction mixture was stirred at 25 °C for 3 h. The mixture was filtered through Celite, evaporated under reduced pressure, and purified using silica column chromatography (5:1 hexanes:EtOAc). The ratio of products **10** and **11** was obtained by comparing the ^{1}H NMR integral values of the two signals at δ 6.59 (d, J = 1.9 Hz, 1H, **10**), 4.75 (d, J = 1.5 Hz, 1H, **11**).

COMPUTATIONAL METHODS

DFT calculations were performed using the Gaussian 09 software package[67] with the BP86 functional.[68] Main group elements were described using the 6-31+G(d) Pople basis set as implemented in Gaussian 09.[69] Gold was described using the relativistic core potential and valence basis set combination of Stevens et al.,[70] denoted CEP-31G in Gaussian09. This choice of methods was based upon results of a benchmark study performed on a model of complex **5c** (see the Supporting Information) and on published studies demonstrating that the BP86 functional with similar basis sets reliably models key structural features of related gold(I) complexes.[71] Dispersion-corrected calculations utilized Grimme's D3 dispersion correction.[53] All geometry optimizations were conducted in the gas phase and were validated through frequency calculations, which verified the structures as energetic minima with no imaginary frequencies. Noncovalent interaction plots were generated from calculated electron densities using NCIPLOT 3.0,[55-56] and visualized using VMD[72] at an isovalue of 0.5.

Percent buried volumes ($\%V_{bur}$)[27c,50] and steric maps[51b] were calculated using SambVca 2.0[51a] with the following input parameters and options: Bondi radii scaled by 1.17, sphere radius 3.5 Å, mesh spacing for numerical integration 0.05, hydrogen atoms omitted. All $\%V_{bur}$ calculations used the crystallographic Au-$C_{carbene}$ distances in order to account for the effect of variations in metal-ligand distance on steric shielding.

ASSOCIATED CONTENT

Supporting Information

Crystal data for structurally characterized compounds (CCDC deposition numbers 1945190-1945201), additional details of DFT calculations, Cartesian coordinates of DFT-optimized geometries, supplemental figures, and copies of ^{1}H and ^{13}C and NMR spectra.

This material is available free of charge via the Internet at http://pubs.acs.org.

AUTHOR INFORMATION

Corresponding Author

*E-mail: legrande@unt.edu

Notes

§Current address: Department of Chemistry, University of Louisville, Louisville, KY, USA

ACKNOWLEDGMENT

We gratefully acknowledge the National Science Foundation (CHE-1360610) for financial support of this research. Prof. Andrés Cisneros, Erik Vazquez Montelongo, and Matt Tiemann (UNT) are thanked for helpful discussions and assistance with computational studies. Prof. Joshua Figueroa (UC San Diego) is acknowledged for generously donating a sample of $CNAr^{Dipp2}$ (**11**). Eric Reinheimer (Rigaku Oxford) provided assistance with data collection and refinement for some of the X-ray structures. We acknowledge the National Science Foundation MRI Program and the University of North Texas for supporting the acquisition of high-performance computing infrastructure (CHE-1531468) and a Rigaku XtaLAB Synergy-S X-ray diffractometer (CHE-1726652).

REFERENCES

(1) (a) Hashmi, A. S. K.; Rudolph, M. *Chem. Soc. Rev.* **2008**, *37*, 1766-1775. (b) Fürstner, A. *Chem. Soc. Rev.* **2009**, *38*, 3208-3221. (c) Shapiro, N. D.; Toste, F. D. *Synlett* **2010**, *5*, 675-691. (d) Krause, N.; Winter, C. *Chem. Rev.* **2011**, *111*, 1994-2009. (e) Corma, A.; Leyva-Pérez, A.; Sabater, M. J. *Chem. Rev.* **2011**, *111*, 1657-1712. (f) *Modern Gold Catalyzed Synthesis*; Hashmi, A. S. K.; Toste, F. D., Eds.; Wiley-VCH: Weinheim, 2012. (g) Rudolph, M.; Hashmi, A. S. K. *Chem. Soc. Rev.* **2012**, *41*, 2448-2462. (h) *Top. Curr. Chem. 357: Homogeneous Gold Catalysis*; Slaughter, L. M., Ed.; Springer, 2014. (i) Dorel, R.; Echavarren, A. M. *Chem. Rev.* **2015**, *115*, 9028-9072.

(2) (a) Jiménez-Núñez, E.; Echavarren, A. M. *Chem. Rev.* **2008**, *108*, 3326-3350. (b) Obradors, C.; Echavarren, A. M. *Chem. Commun.* **2014**, *50*, 16-28. (c) Fensterbank, L.; Malacria, M. *Acc. Chem. Res.* **2014**, *47*, 953-965.

(3) Wei, Y.; Shi, M. *ACS Catal.* **2016**, *6*, 2515-2524.

(4) Mahatthananchai, J.; Dumas, A. M.; Bode, J. W. *Angew. Chem. Int. Ed.* **2012**, *51*, 10954-10990.

(5) For reviews of ligand effects in regiodivergent gold catalysis, see: (a) Gorin, D. J.; Sherry, B. D.; Toste, F. D. *Chem. Rev.* **2008**, *108*, 3351-3378. (b) Gatineau, D.; Goddard, J.-P.; Mouriès-Mansuy, V.; Fensterbank, L. *Isr. J. Chem.* **2013**, *53*, 892-900. (c) Wang, Y.-M.; Lackner, A. D.; Toste, F. D. *Acc. Chem. Res.* **2014**, *47*, 889-901.

(6) For selected examples of ligand effect in regiodivergent gold catalysis, see: (a) Marion, N.; de Fremont, P.; Lemiere, G.; Stevens, E. D.; Fensterbank, L.; Malacria, M.; Nolan, S. P. *Chem. Commun.* **2006**, 2048-2050. (b) Ferrer, C.; Amijs, C. H. M.; Echavarren, A. M. *Chem. Eur. J.* **2007**, *13*, 1358-1373. (c) Amijs, C. H. M.; Ferrer, C.; Echavarren, A. M. *Chem. Commun.* **2007**, 698-700. (d) Amijs, C. H. M.; López-Carrillo, V.; Raducan, M.; Pérez-Galán, P.; Ferrer, C.; Echavarren, A. M. *J. Org. Chem.* **2008**, *73*, 7721-7730. (e) Mauleón, P.; Zeldin, R. M.; González, A. Z.; Toste, F. D. *J. Am. Chem. Soc.* **2009**, *131*, 6348-6349. (f) Alcarazo, M.; Stork, T.; Anoop, A.; Thiel, W.; Fürstner, A. *Angew. Chem. Int. Ed.* **2010**, *49*, 2542-2546. (g) Alonso, I.; Trillo, B.; López, F.; Montserrat, S.; Ujaque, G.; Castedo, L.; Lledós, A.; Mascareñas, J. L. *J. Am. Chem. Soc.* **2009**, *131*, 13020-13030. (h) Barabé, F.; Levesque, P.; Korobkov, I.; Barriault, L. *Org. Lett.* **2011**, *13*, 5580-5583. (i) Barluenga, J.; Sigüeiro, R.; Vicente, R.; Ballesteros, A.; Tomás, M.; Rodríguez, M. A. *Angew. Chem. Int. Ed.* **2012**, *51*, 10377-10381. (j) Carreras, J.; Gopakumar, G.; Gu, L.; Gimeno, A.; Linowski, P.; Petuškova, J.; Thiel, W.; Alcarazo, M. *J. Am. Chem. Soc.* **2013**, *135*, 18815-18823. (k) Tudela, E.; González, J.; Vicente, R.; Santamaría, J.; Rodríguez, M. A.; Ballesteros, A. *Angew. Chem. Int. Ed.* **2014**, *53*, 12097-12100. (l) Handa, S.; Subramanium, S. S.; Ruch, A. A.; Tanski, J. M.; Slaughter, L. M. *Org. Biomol. Chem.* **2015**, *13*, 3936-3949. (m) Mei, L.-Y.; Wei, Y.; Tang, X.-Y.; Shi, M. *J. Am. Chem. Soc.* **2015**, *137*, 8131-8137. (n) Rao, W.; Susanti, D.; Ayers, B. J.; Chan, P. W. H. *J. Am. Chem. Soc.* **2015**, *137*, 6350-6355. (o) Ding, D.; Mou, T.; Feng, M.; Jiang, X. *J. Am. Chem. Soc.* **2016**, *138*, 5218-5221.

(7) For elegant studies of ligand electronic effects on *activity* (i.e., TOF) in gold catalysis, see: (a) Wang, W.; Hammond, G. B.; Xu, B. *J. Am. Chem. Soc.* **2012**, *134*, 5697-5705. (b) Gaggioli, C. A.; Ciancaleoni, G.; Biasiolo, L.; Bistoni, G.; Zuccaccia, D.; Belpassi, L.; Belanzoni, P.; Tarantelli, F. *Chem. Commun.* **2015**, *51*, 5990-5993. (c) Gaggioli, C. A.; Ciancaleoni, G.; Zuccaccia, D.; Bistoni, G.; Belpassi, L.; Tarantelli, F.; Belanzoni, P. *Organometallics* **2016**, *35*, 2275-2285.

(8) Christian, A. H.; Niemeyer, Z. L.; Sigman, M. S.; Toste, F. D. *ACS Catalysis* **2017**, *7*, 3973-3978.

(9) For studies of the interplay of counterion and ligand effects on *activity* (but not selectivity) of gold catalysts, see: (a) Biasiolo, L.; Ciancaleoni, G.; Belpassi, L.; Bistoni, G.; Macchioni, A.; Tarantelli, F.; Zuccaccia, D. *Catal. Sci. Technol.* **2015**, *5*, 1558-1567. (b) Biasiolo, L.; Del Zotto, A.; Zuccaccia, D. *Organometallics* **2015**, *34*, 1759-1765.

(10) For studies of counterion electrostatic effects on regioselectivity in gold catalysis, see: (a) Lau, V. M.; Gorin, C. F.; Kanan, M. W. *Chem. Sci.* **2014**, *5*, 4975-4979. (b) Lau, V. M.; Pfalzgraff, W. C.; Markland, T. E.; Kanan, M. W. *J. Am. Chem. Soc.* **2017**, *139*, 4035-4041.

(11) For reviews of ADC ligands in catalysis, see: (a) Slaughter, L. M. *ACS Catal.* **2012**, *2*, 1802-1816. (b) Slaughter, L. M. In *N-Heterocyclic Carbenes: Effective Tools for Organometallic Synthesis*; Nolan, S. P., Ed.; Wiley-VCH: Weinheim, 2014. (c) Boyarskiy, V. P.; Luzyanin, K. V.; Kukushkin, V. Y. *Coord. Chem. Rev.* **2012**, *256*, 2029-2056.

(12) (a) Slaughter, L. M. *Comments Inorg. Chem.* **2008**, *29*, 46-72. (b) Boyarskiy, V. P.; Bokach, N. A.; Luzyanin, K. V.; Kukushkin, V. Y. *Chem. Rev.* **2015**, *115*, 2698-2779.

(13) (a) Moncada, A. I.; Manne, S.; Tanski, J. M.; Slaughter, L. M. *Organometallics* **2006**, *25*, 491-505. (b) Luzyanin, K. V.; Tskhovrebov, A. G.; Carias, M. C.; Guedes da Silva, M. F. C.; Pombeiro, A. J. L.; Kukushkin, V. Y. *Organometallics* **2009**, *28*, 6559-6566. (c) Hashmi, A. S. K.; Lothschütz, C.; Böhling, C.; Rominger, F. *Organometallics* **2011**, *30*, 2411-2417. (d) Owusu, M. O.; Handa, S.; Slaughter, L. M. *Appl. Organomet. Chem.* **2012**, *26*, 712-717. (e) Kinzhalov, M. A.; Luzyanin, K. V.; Boyarskiy, V. P.; Haukka, M.; Kukushkin, V. Y. *Organometallics* **2013**, *32*, 5212-5223. (f) Valishina, E. A.; Silva, M. F. C. G. d.; Kinzhalov, M. A.; Timofeeva, S. A.; Buslaeva, T. M.; Haukka, M.; Pombeiro, A. J. L.; Boyarskiy, V. P.; Kukushkin, V. Y.; Luzyanin, K. V. *J. Mol. Catal. A: Chem.* **2014**, *395*, 162-171.

(14) (a) Bartolomé, C.; Ramiro, Z.; Pérez-Galán, P.; Bour, C.; Raducan, M.; Echavarren, A. M.; Espinet, P. *Inorg. Chem.* **2008**, *47*, 11391-11397. (b) Bartolomé, C.; Ramiro, Z.; García-Cuadrado, D.; Pérez-Galán, P.; Raducan, M.; Bour, C.; Echavarren, A. M.; Espinet, P. *Organometallics* **2010**, *29*, 951-956. (c) Bartolomé, C.; García-Cuadrado, D.; Ramiro, Z.; Espinet, P. *Inorg. Chem.* **2010**, *49*, 9758-9764. (d) Hashmi, A. S. K.; Hengst, T.; Lothschütz, C.; Rominger, F. *Adv. Synth. Catal.* **2010**, *352*, 1315-1337. (e) Wang, Y.-M.; Kuzniewski, C. N.; Rauniyar, V.; Hoong, C.; Toste, F. D. *J. Am. Chem. Soc.* **2011**, *133*, 12972-12975. (f) Handa, S.; Slaughter, L. M. *Angew. Chem. Int. Ed.* **2012**, *51*, 2912-2915. (g) Khrakovsky, D. A.; Tao, C.; Johnson, M. W.; Thornbury, R. T.; Shevick, S. L.; Toste, F. D. *Angew. Chem. Int. Ed.* **2016**, *55*, 6079-6083. (h) Niemeyer, Z. L.; Pindi, S.; Khrakovsky, D. A.; Kuzniewski, C. N.; Hong, C. M.; Joyce, L. A.; Sigman, M. S.; Toste, F. D. *J. Am. Chem. Soc.* **2017**, *139*, 12943-12946.

(15) Michelin, R. A.; Pombeiro, A. J. L.; Guedes da Silva, M. F. C. *Coord. Chem. Rev.* **2001**, *218*, 75-112.

(16) Seo, H.; Roberts, B. P.; Abboud, K. A.; Merz, K. M., Jr.; Hong, S. *Org. Lett.* **2010**, *12*, 4860-4863.

(17) For other notable examples of catalysis with isocyanide-derived ADC ligands, see: (a) Moncada, A. I.; Khan, M. A.; Slaughter, L. M. *Tetrahedron Lett.* **2005**, *46*, 1399-1403. (b) Wanniarachchi, Y. A.;

Kogiso, Y.; Slaughter, L. M. *Organometallics* **2008**, *27*, 21-24. (c) Wanniarachchi, Y. A.; Subramanium, S. S.; Slaughter, L. M. *J. Organomet. Chem.* **2009**, *694*, 3297-3305. (d) Bartolomé, C.; García-Cuadrado, D.; Ramiro, Z.; Espinet, P. *Organometallics* **2010**, *29*, 3589-3592. (e) Hashmi, A. S. K.; Bührle, M.; Wölfle, M.; Rudolph, M.; Wieteck, M.; Rominger, F.; Frey, W. *Chem. Eur. J.* **2010**, *16*, 9846-9854. (f) Tskhovrebov, A. G.; Luzyanin, K. V.; Kuznetsov, M. L.; Sorokoumov, V. N.; Balova, I. A.; Haukka, M.; Kukushkin, V. Y. *Organometallics* **2011**, *30*, 863-874. (g) Chay, R. S.; Luzyanin, K. V.; Kukushkin, V. Y.; Guedes da Silva, M. F. C.; Pombeiro, A. J. L. *Organometallics* **2012**, *31*, 2379-2387. (h) Blanco Jaimes, M. C.; Böhling, C. R. N.; Serrano-Becerra, J. M.; Hashmi, A. S. K. *Angew. Chem. Int. Ed.* **2013**, *52*, 7963-7966. (i) Miltsov, S.; Karavan, V.; Boyarsky, V.; Gómez-de Pedro, S.; Alonso-Chamarro, J.; Puyol, M. *Tetrahedron Lett.* **2013**, *54*, 1202-1204. (j) Knorn, M.; Lutsker, E.; Reiser, O. *Organometallics* **2015**, *34*, 4515-4520. (k) Mikhaylov, V. N.; Sorokoumov, V. N.; Korvinson, K. A.; Novikov, A. S.; Balova, I. A. *Organometallics* **2016**, *35*, 1684-1697.

(18) For examples of catalysis with ADC ligands prepared by other routes, see: (a) Kremzow, D.; Seidel, G.; Lehmann, C. W.; Fürstner, A. *Chem. Eur. J.* **2005**, *11*, 1833-1853. (b) Dhudshia, B.; Thadani, A. N. *Chem. Commun.* **2006**, 668-670. (c) Snead, D. R.; Ghiviriga, I.; Abboud, K. A.; Hong, S. *Org. Lett.* **2009**, *11*, 3274-3277. (d) Snead, D. R.; Inagaki, S.; Abboud, K. A.; Hong, S. *Organometallics* **2010**, *29*, 1729-1739. (e) Rosen, E. L.; Sung, D. H.; Chen, Z.; Lynch, V. M.; Bielawski, C. W. *Organometallics* **2010**, *29*, 250-256.

(19) (a) Jahnke, M. C.; Hahn, F. E. *Top. Organomet. Chem.* **2010**, *30*, 95-129. (b) *N-Heterocyclic Carbenes: Effective Tools for Organometallic Synthesis*; Nolan, S. P., Ed.; Wiley-VCH: Weinheim, 2014.

(20) (a) Alder, R. W.; Blake, M. E.; Oliva, J. M. *J. Phys. Chem. A* **1999**, *103*, 11200-11211. (b) Denk, K.; Sirsch, P.; Herrmann, W. A. *J. Organomet. Chem.* **2002**, *649*, 219-224.

(21) (a) Back, O.; Henry-Ellinger, M.; Martin, C. D.; Martin, D.; Bertrand, G. *Angew. Chem. Int. Ed.* **2013**, *52*, 2939-2943. (b) Liske, A.; Verlinden, K.; Buhl, H.; Schaper, K.; Ganter, C. *Organometallics* **2013**, *32*, 5269-5272.

(22) Martin, D.; Canac, Y.; Lavallo, V.; Bertrand, G. *J. Am. Chem. Soc.* **2014**, *136*, 5023-5030.

(23) Johansson, M. J.; Gorin, D. J.; Staben, S. T.; Toste, F. D. *J. Am. Chem. Soc.* **2005**, *127*, 18002-18003.

(24) (a) Benitez, D.; Tkatchouk, E.; Gonzalez, A. Z.; Goddard, W. A.; Toste, F. D. *Org. Lett.* **2009**, *11*, 4798-4801. (b) Ye, L.; Wang, Y.; Aue, D. H.; Zhang, L. *J. Am. Chem. Soc.* **2012**, *134*, 31-34.

(25) (a) Malhotra, D.; Mashuta, M. S.; Hammond, G. B.; Xu, B. *Angew. Chem. Int. Ed.* **2014**, *53*, 4456-4459. (b) Ebule, R. E.; Malhotra, D.; Hammond, G. B.; Xu, B. *Adv. Synth. Catal.* **2016**, *358*, 1478-1481.

(26) Brown, T. J.; Weber, D.; Gagné, M. R.; Widenhoefer, R. A. *J. Am. Chem. Soc.* **2012**, *134*, 9134-9137.

(27) (a) de Frémont, P.; Scott, N. M.; Stevens, E. D.; Nolan, S. P. *Organometallics* **2005**, *24*, 2411-2418. (b) Fructos, M. R.; Belderrain, T. R.; de Frémont, P.; Scott, N. M.; Nolan, S. P.; Díaz-Requejo, M. M.; Pérez, P. J. *Angew. Chem. Int. Ed.* **2005**, *44*, 5284-5288. (c) Clavier, H.; Nolan, S. P. *Chem. Commun.* **2010**, *46*, 841-861.

(28) All $\%V_{bur}$ parameters reported in this paper were calculated from the crystal structures of the (carbene)Au-Cl complexes, as described in the Computational Methods section.

(29) (a) Bender, C. F.; Widenhoefer, R. A. *Org. Lett.* **2006**, *8*, 5303-5305. (b) López, S.; Herrero-Gómez, E.; Pérez-Galán, P.; Nieto-Oberhuber, C.; Echavarren, A. M. *Angew. Chem., Int. Ed.* **2006**, *45*, 6029-6032. (c) Marion, N.; Ramón, R. S.; Nolan, S. P. *J. Am. Chem. Soc.* **2009**, *131*, 448-449. (d) Huguet, N.; Lebœuf, D.; Echavarren, A. M. *Chem. - Eur. J.* **2013**, *19*, 6581-6585.

(30) López-Carrillo, V.; Huguet, N.; Mosquera, Á.; Echavarren, A. M. *Chem. - Eur. J.* **2011**, *17*, 10972-10978.

(31) (a) Berthon-Gelloz, G.; Siegler, M. A.; Spek, A. L.; Tinant, B.; Reek, J. N. H.; Markó, I. E. *Dalton Trans.* **2010**, *39*, 1444-1446. (b) Gómez-Suárez, A.; Ramón, R. S.; Songis, O.; Slawin, A. M. Z.; Cazin, C. S. J.; Nolan, S. P. *Organometallics* **2011**, *30*, 5463-5470.

(32) (a) Weber, S. G.; Rominger, F.; Straub, B. F. *Eur. J. Inorg. Chem.* **2012**, *2012*, 2863-2867. (b) Weber, S. G.; Zahner, D.; Rominger, F.; Straub, B. F. *ChemCatChem* **2013**, *5*, 2330-2335.

(33) Roy, M. M. D.; Lummis, P. A.; Ferguson, M. J.; McDonald, R.; Rivard, E. *Chem. – Eur. J.* **2017**, *23*, 11249-11252.

(34) Frey, G. D.; Dewhurst, R. D.; Kousar, S.; Donnadieu, B.; Bertrand, G. *J. Organomet. Chem.* **2008**, *693*, 1674-1682.

(35) (a) Gómez-Suárez, A.; Oonishi, Y.; Meiries, S.; Nolan, S. P. *Organometallics* **2013**, *32*, 1106-1111. (b) Izquierdo, F.; Manzini, S.; Nolan, S. P. *Chem. Commun.* **2014**, *50*, 14926-14937. (c) Brill, M.; Collado, A.; Cordes, D. B.; Slawin, A. M. Z.; Vogt, M.; Grützmacher, H.; Nolan, S. P. *Organometallics* **2015**, *34*, 263-274. (d) Collado, A.; Patrick, S. R.; Gasperini, D.; Meiries, S.; Nolan, S. P. *Beilstein J. Org. Chem.* **2015**, *11*, 1809-1814.

(36) For related bulky acyclic aminooxycarbene ligands, see: Seo, H.; Snead, D. R.; Abboud, K. A.; Hong, S. *Organometallics* **2011**, *30*, 5725-5730.

(37) (a) Alder, R. W.; Blake, M. E. *Chem. Commun.* **1997**, 1513-1514. (b) Alder, R. W.; Chaker, L.; Paolini, F. P. V. *Chem. Commun.* **2004**, 2172-2173. (c) Alder, R. W.; Blake, M. E.; Chaker, L.; Harvey, J. N.; Paolini, F.; Schütz, J. *Angew. Chem., Int. Ed.* **2004**, *43*, 5896-5911. (d) Otto, M.; Coejero, S.; Canac, Y.; Romanenko, V. D.; Rudzevitch, V.; Bertrand, G. *J. Am. Chem. Soc.* **2004**, *126*, 1016-1017.

(38) (a) Alder, R. W.; Allen, P. R.; Murray, M.; Orpen, A. G. *Angew. Chem. Int. Ed.* **1996**, *35*, 1121-1123. (b) Schulz, T.; Leibold, M.; Färber, C.; Maurer, M.; Porsch, T.; Holthausen, M. C.; Siemeling, U. *Chem. Commun.* **2012**, *48*, 9123-9125.

(39) Alder, R. W.; Blake, M. E.; Bufali, S.; Butts, C. P.; Orpen, A. G.; Schütz, J.; Williams, S. J. *J. Chem. Soc., Perkin Trans. 1* **2001**, 1586-1593.

(40) Rosen, E. L.; Sanderson, M. D.; Saravanakumar, S.; Bielawski, C. W. *Organometallics* **2007**, *26*, 5774-5777.

(41) (a) Johnson, B. V.; Shade, J. E. *J. Organomet. Chem.* **1979**, *179*, 357-366. (b) Moncada, A. I.; Tanski, J. M.; Slaughter, L. M. *J. Organomet. Chem.* **2005**, *690*, 6247-6251. (c) Wanniarachchi, Y. A.; Slaughter, L. M. *Organometallics* **2008**, *27*, 1055-1062.

(42) (a) Surry, D. S.; Buchwald, S. L. *Angew. Chem. Int. Ed.* **2008**, *47*, 6338-6361. (b) Pérez-Galán, P.; Delpont, N.; Herrero-Gómez, E.; Maseras, F.; Echavarren, A. M. *Chem. Eur. J.* **2010**, *16*, 5324-5332.

(43) (a) Twamley, B.; Haubrich, S. T.; Power, P. P. *Adv. Organomet. Chem.* **1999**, *44*, 1-65. (b) Clyburne, J. A. C.; McMullen, N. *Coord. Chem. Rev.* **2000**, *210*, 73-99. (c) Ni, C.; Power, P. P. *Struct. Bond.* **2010**, *136*, 59-112.

(44) Tanabiki, M.; Tsuchiya, K.; Kumanomido, Y.; Matsubara, K.; Motoyama, Y.; Nagashima, H. *Organometallics* **2004**, *23*, 3976-3981.

(45) (a) Fox, B. J.; Sun, Q. Y.; DiPasquale, A. G.; Fox, A. R.; Rheingold, A. L.; Figueroa, J. S. *Inorg. Chem.* **2008**, *47*, 9010-9020. (b) Fox, B. J.; Millard, M. D.; DiPasquale, A. G.; Rheingold, A. L.; Figueroa, J. S. *Angew. Chem., Int. Ed.* **2009**, *48*, 3473-3477, S3473/1-S3473/19. (c) Labios, L. A.; Millard, M. D.; Rheingold, A. L.; Figueroa, J. S. *J. Am. Chem. Soc.* **2009**, *131*, 11318-11319. (d) Ditri, T. B.; Fox, B. J.; Moore, C. E.; Rheingold, A. L.; Figueroa, J. S. *Inorg. Chem.* **2009**, *48*, 8362-8375. (e) Margulieux, G. W.; Weidemann, N.; Lacy, D. C.; Moore, C. E.; Rheingold, A. L.; Figueroa, J. S. *J. Am. Chem. Soc.* **2010**, *132*, 5033-5035. (f) Stewart, M. A.; Moore, C. E.; Ditri, T. B.; Labios, L. A.; Rheingold, A. L.; Figueroa, J. S. *Chem. Commun.* **2011**, *47*, 406-408. (g) Emerich, B. M.; Moore, C. E.; Fox, B. J.; Rheingold, A. L.; Figueroa, J. S. *Organometallics* **2011**, *30*, 2598-2608. (h) Ditri, T. B.; Moore, C. E.; Rheingold, A. L.; Figueroa, J. S. *Inorg. Chem.* **2011**, *50*, 10448-10459. (i) Carpenter, A. E.; Margulieux, G. W.; Millard, M. D.; Moore, C. E.; Weidemann, N.; Rheingold, A. L.; Figueroa, J. S. *Angew. Chem., Int. Ed.* **2012**, *51*, 9412-9416. (j) Ditri, T. B.; Carpenter, A. E.; Ripatti, D. S.; Moore, C. E.; Rheingold, A. L.; Figueroa, J. S. *Inorg. Chem.* **2013**, *52*, 13216-13229. (k) Mokhtarzadeh, C. C.; Margulieux, G. W.; Carpenter, A. E.; Weidemann, N.; Moore, C. E.; Rheingold, A. L.; Figueroa, J. S. *Inorg. Chem.* **2015**, *54*, 5579-5587. (l) Agnew, D. W.; Moore, C. E.; Rheingold, A. L.; Figueroa, J. S. *Angew. Chem., Int. Ed.* **2015**, *54*, 12673-12677. (m) Carpenter, A. E.; Rheingold, A. L.; Figueroa, J. S. *Organometallics* **2016**, *35*, 2309-2318. (n) Mokhtarzadeh, C. C.; Rheingold, A. L.; Figueroa, J. S. *Dalton Trans.* **2016**, *45*, 14561-14569.

(46) Uson, R.; Laguna, A.; Laguna, M. *Inorg. Synth.* **1989**, *26*, 85-91.
(47) Schmidbaur, H.; Schier, A. *Chem. Soc. Rev.* **2008**, *37*, 1931-1951.
(48) For a similar tetrameric structure, see: Guy, J. J.; Jones, P. G.; Mays, M. J.; Sheldrick, G. M. *J. Chem. Soc., Dalton Trans.* **1977**, 8-10.
(49) Leung, C. H.; Incarvito, C. D.; Crabtree, R. H. *Organometallics* **2006**, *25*, 6099-6107.
(50) Hillier, A. C.; Sommer, W. J.; Yong, B. S.; Peterson, J. L.; Cavallo, L.; Nolan, S. P. *Organometallics* **2003**, *22*, 4322-4326.
(51) (a) Falivene, L.; Credendino, R.; Poater, A.; Petta, A.; Serra, L.; Oliva, R.; Scarano, V.; Cavallo, L. *Organometallics* **2016**, *35*, 2286-2293. (b) Gómez-Suárez, A.; Nelson, D. J.; Nolan, S. P. *Chem. Commun.* **2017**, *53*, 2650-2660.
(52) Nishio, M.; Hirota, M.; Umezawa, Y. *The CH/π Interaction: Evidence, Nature, and Consequences*; Wiley-VCH: New York, 1998.
(53) Grimme, S.; Antony, J.; Ehrlich, S.; Krieg, H. *J. Chem. Phys.* **2010**, *132*, 154104.
(54) (a) Grimme, S.; Djukic, J.-P. *Inorg. Chem.* **2011**, *50*, 2619-2628. (b) Ehrlich, S.; Bettinger, H. F.; Grimme, S. *Angew. Chem. Int. Ed.* **2013**, *52*, 10892-10895. (c) Guo, J.-D.; Liptrot, D. J.; Nagase, S.; Power, P. P. *Chem. Sci.* **2015**, *6*, 6235-6244. (d) Schweighauser, L.; Strauss, M. A.; Bellotto, S.; Wegner, H. A. *Angew. Chem. Int. Ed.* **2015**, *54*, 13436-13439.
(55) Johnson, E. R.; Keinan, S.; Mori-Sánchez, P.; Contreras-García, J.; Cohen, A. J.; Yang, W. *J. Am. Chem. Soc.* **2010**, *132*, 6498-6506.
(56) Contreras-García, J.; Johnson, E. R.; Keinan, S.; Chaudret, R.; Piquemal, J.-P.; Beratan, D. N.; Yang, W. *J. Chem. Theory Comput.* **2011**, *7*, 625-632.
(57) Blanco-Díaz, E. G.; Vázquez-Montelongo, E. A.; Cisneros, G. A.; Castrejón-González, E. O. *J. Chem. Phys.* **2018**, *148*, 054303.
(58) Forlani, L.; Lunazzi, L.; Medici, A. *Tetrahedron Lett.* **1977**, *18*, 4525-4526.
(59) Hunter, C. A.; Sanders, J. K. M. *J. Am. Chem. Soc* **1990**, *112*, 5525-5534.
(60) Arumugam, K.; Varghese, B.; Brantley, J. N.; Konda, S. S. M.; Lynch, V. M.; Bielawski, C. W. *Eur. J. Org. Chem.* **2014**, 493-497.
(61) For relevant discussions, see: (a) Benitez, D.; Shapiro, N. D.; Tkatchouk, E.; Wang, Y.; Goddard Iii, W. A.; Toste, F. D. *Nat. Chem.* **2009**, *1*, 482. (b) Wang, Y.; Muratore, M. E.; Echavarren, A. M. *Chem. – Eur. J.* **2015**, *21*, 7332-7339. (c) Harris, R. J.; Widenhoefer, R. A. *Chem. Soc. Rev.* **2016**, *45*, 4533-4551.
(62) Jover, J.; Fey, N.; Harvey, J. N.; Lloyd-Jones, G. C.; Orpen, A. G.; Owen-Smith, G. J. J.; Murray, P.; Hose, D. R. J.; Osborne, R.; Purdie, M. *Organometallics* **2010**, *29*, 6245-6258.
(63) Brauer, G. *Handbuch der Präparativen Anorganischen Chemie, Vol. 2, 3rd ed.*; Verlag: Stuttgart, 1978, p 1014.
(64) Gao, H.-y.; Liu, F.-s.; Hu, H.-b.; Zhu, F.-m.; Wu, Q. *Chin. J. Polym. Sci.* **2013**, *31*, 563-573.
(65) Nevado, C.; Charruault, L.; Michelet, V.; Nieto-Oberhuber, C.; Munoz, M. P.; Mendez, M.; Rager, M.-N.; Genet, J.-P.; Echavarren, A. M. *Eur. J. Org. Chem.* **2003**, 706-713.
(66) Fulmer, G. R.; Miller, A. J. M.; Sherden, N. H.; Gottlieb, H. E.; Nudelman, A.; Stoltz, B. M.; Bercaw, J. E.; Goldberg, K. I. *Organometallics* **2010**, *29*, 2176-2179.
(67) Frisch, M. J.; Trucks, G. W.; Schlegel, H. B.; Scuseria, G. E.; Robb, M. A.; Cheeseman, J. R.; Scalmani, G.; Barone, V.; Mennucci, B.; Petersson, G. A.; Nakatsuji, H.; Caricato, M.; Li, X.; Hratchian, H. P.; Izmaylov, A. F.; Bloino, J.; Zheng, G.; Sonnenberg, J. L.; Hada, M.; Ehara, M.; Toyota, K.; Fukuda, R.; Hasegawa, J.; Ishida, M.; Nakajima, T.; Honda, Y.; Kitao, O.; Nakai, H.; Vreven, T.; Montgomery Jr., J. A.; Peralta, J. E.; Ogliaro, F.; Bearpark, M. J.; Heyd, J.; Brothers, E. N.; Kudin, K. N.; Staroverov, V. N.; Kobayashi, R.; Normand, J.; Raghavachari, K.; Rendell, A. P.; Burant, J. C.; Iyengar, S. S.; Tomasi, J.; Cossi, M.; Rega, N.; Millam, N. J.; Klene, M.; Knox, J. E.; Cross, J. B.; Bakken, V.; Adamo, C.; Jaramillo, J.; Gomperts, R.; Stratmann, R. E.; Yazyev, O.; Austin, A. J.; Cammi, R.; Pomelli, C.; Ochterski, J. W.; Martin, R. L.; Morokuma, K.; Zakrzewski, V. G.; Voth, G. A.; Salvador, P.; Dannenberg, J. J.; Dapprich, S.; Daniels, A. D.; Farkas, Ö.; Foresman, J. B.; Ortiz, J. V.; Cioslowski, J.; Fox, D. J. *Gaussian 09, Revision D.01*; Gaussian, Inc.: Wallingford, CT, USA, 2009.
(68) (a) Perdew, J. P. *Phys. Rev. B* **1986**, *33*, 8822-8824. (b) Becke, A. D. *Phys. Rev. A* **1988**, *38*, 3098-3100.
(69) (a) Hehre, W. J.; Ditchfield, R.; Pople, J. A. *J. Chem. Phys.* **1972**, *56*, 2257-2261. (b) Hariharan, P. C.; Pople, J. A. *Theor. Chim. Acta* **1973**, *28*, 213-222. (c) Hariharan, P. C.; Pople, J. A. *Mol. Phys.* **1974**, *27*, 209-214.
(70) Krauss, M.; Stevens, W. J.; Basch, H.; Jasien, P. G. *Can. J. Chem.* **1992**, *70*, 612-630.
(71) (a) Nemcsok, D.; Wichmann, K.; Frenking, G. *Organometallics* **2004**, *23*, 3640-3646. (b) Faza, O. N.; López, C. S. *Top. Curr. Chem.* **2015**, *357*, 213-283.
(72) Humphrey, W.; Dalke, A.; Schulten, K. *J. Mol. Graphics* **1996**, *14*, 33-38.

TOC Graphic Entry